



University of
BRISTOL

Propagation Modelling using Iterative Physical Optics

Student Name: Ioannis Mavromatis

Supervisor Name: Prof. Christopher Railton

A dissertation submitted to the University of Bristol in accordance with the requirements of the degree of MSc in Wireless Communications and Signal Processing in the Faculty of Engineering.

Department of Electrical and Electronic Engineering

Date: 19 September 2014

Word Count: 13182

Abstract

Ray tracing, Finite-Difference Time-Domain, Shooting and Bouncing Ray, and Generalised Ray Expansion are techniques that can model the wave propagation in a specific site. Although, these techniques work well, they exhibit some drawbacks that Iterative Physical Optics (IPO) technique can overcome. IPO can predict the wave propagation, by using the surface current of an object based on Kirchhoff approximation.

In this project, IPO will be used and implemented in a software written in Pascal language, subsequently of a previous embodiment, and an indoor propagation scenario will be simulated. IPO will be combined with FDTD and an analytical method, creating two hybrid methods for predicting the wave propagation. Walls and other objects acting as obstacles inside a building, are discrete into smaller objects such as bricks that show a periodic pattern. This feature will be exploited, and by the usage of the previously mentioned methods, the radiation of a ray inside an object will be calculated. The results will be used from the IPO algorithm to calculate the energy arriving at the receiver propagating through a complex lossy structure.

The drawbacks and the shortages of the previous software will be implemented at first. The simulated results will be compared with measured results, coming from experiments conducted from the University of Bristol. In addition to that, the code will be optimised to increase the performance of the simulator. The results from the simulations show, that both hybrid techniques predict accurately the propagation characteristics. Using the analytical method, the accuracy is increased because a more complex structure is taken into account.

Dedication and Acknowledgements

My sincere thanks to my supervisor, Prof. Christopher Railton, for his valuable guidance on my project. I thank him for his patience and kindness, his wisdom in the related area of my project and his help with all the issues that came up during my project.

DECLARATION AND DISCLAIMER

I declare that the work in this dissertation was carried out in accordance with the requirements of the University's Regulations and Code of Practice for Taught Postgraduate Programmes and that it has not been submitted for any other academic award.

Except where indicated by specific reference in the text, this work is my own work. Work done in collaboration with, or with the assistance of others, is indicated as such. I have identified all material in this dissertation, which is not my own work through appropriate referencing and acknowledgement. Where I have quoted from the work of others, I have included the source in the references/bibliography.

Any views expressed in the dissertation are those of the author.

The author confirms that the printed copy and the electronic version of this thesis are identical.

Signed:

Date: 19 September 2014

Table of Contents

Abstract	i
1) Introduction	1
1.1) Aim	2
1.2) Objectives	2
2) Background.....	4
2.1) Ray Tracing (RT)	4
2.2) Finite-Difference Time-Domain (FDTD)	5
2.3) Shooting and Bouncing Ray (SBR).....	5
2.4) Generalized Ray Expansion (GRE).....	6
2.5) Introduction to Iterative Physical Optics (IPO)	6
2.5.1) Advantages and Disadvantages of IPO	6
2.5.2) Kirchhoff Approximation (KA)	7
2.5.3) Iterative Solution	7
2.6) Building Material Properties	8
2.6) Introduction to Pascal	9
3) Introduction to the software.....	11
3.1) Introduction to IPO3 and IPO_AoA software.....	11
3.2) Structures	13
3.2.1) Wall.....	13
3.2.2) Brick.....	14
3.2.3) Cell	15
3.3) Geometry.....	15
3.4) Scattering Results for Different Materials	16
3.4.1) FDTD Simulation.....	16
3.4.2) Analytical Simulation.....	17
4) Iterative Physical Optics Algorithm.....	21
4.1) Line of Sight Relationship.....	21
4.1.1) Solid Geometry	21
4.2) Initialisation of LOS	22
4.3) E-field from source to receiver	23
4.4) Radiation pattern from the transmitter to the bricks	24
4.5) Radiation from brick to brick	25
5) Received Signal (Final Step of IPO algorithm)	28
5.1) Bricks Contributing to the Received Energy Calculation.....	28
5.2) Fiend Intensity and Total Received Energy.....	30
6) Performance Improvement.....	31
6.1) Code Optimisation	31
6.2) Software Convergence	31
7) Results	33
7.1) LOS Link.....	34
7.2) Position 1	35
7.2.1) Measured Results	35
7.2.2) FDTD Method	36
7.2.3) Analytical Method	37
7.2.3.1) Analytical Dataset - 5.15 GHz	37
7.2.3.2) Analytical dataset - 5.35 GHz.....	40
7.3) Position 2	41
7.3.1) FDTD Method	42

7.3.2) Analytical Method	43
7.3.2.1) Analytical Dataset - 5.15GHz	43
7.3.2.2) Analytical Dataset - 5.35GHz	44
7.4) Position 3	45
7.4.1) Analytical Method	45
7.5) Improved Performance.....	46
7.6) Reflection coefficients and Frequency.....	46
8) How to use the software	49
9) Conclusions.....	51
10) Future Work.....	52
References	53

List of Tables

Table 1 - FDTD method's Material Properties.....	17
Table 2 - Building Material Properties for 5.15GHz.	19
Table 3 - Building Material Properties for 5.35GHz.	19

Table of Figures

Figure 1 - Difference of Length Between two Paths Reflected by Roughness [12]	4
Figure 2 - Iterative Process of IPO algorithm	8
Figure 3 – Simple Pascal Program Structure	10
Figure 4 - Lazarus IDE Graphical User Interphase.....	10
Figure 5 – Lower and Higher Coordinates.....	13
Figure 6 - (P, Q, Face) Coordinates and Front/Back Surfaces	14
Figure 7 - Brick Coordinate System, Cells and Centre Cell of the Structure.....	15
Figure 8 - FDTD Simulation Geometry of a Single Brick.....	17
Figure 9 – First LOS situation – Brick-Brick Dist. shorter than Brick-Wall Dist....	21
Figure 10 – 2nd LOS situation – Brick-Brick Dist. Longer than Brick-Wall Dist.	22
Figure 11 - NLOS Situation – Wall intersects between bricks.....	22
Figure 12 - Incident Angle.....	25
Figure 13 - Two bricks' front surfaces facing each other.....	26
Figure 14 - Target Brick – Three Cosine Theorem	29
Figure 15 - IPO Algorithm and Software Applications Implementing it.....	30
Figure 16 - Results Plotted from Two Different Iterations that Overlay	32
Figure 17 - House Layout	33
Figure 18 - LOS link for 5.15GHz.....	34
Figure 19 - LOS link for 5.35GHz.....	34
Figure 20 - Measured Result for Position 1 - 5.15GHz	35
Figure 21 - Measured Result for Position 1 - 5.35GHz	35
Figure 22 - Position 1 – FDTD Dataset Simulation - 5.15GHz.....	36
Figure 23 - Position 1 – FDTD Dataset Simulation - 5.35GHz.....	36
Figure 24 - Position 1 - Larger Brick Simulation - 5.15GHz	37
Figure 25 - Position 1 - Larger Number of Cells Simulation - 5.15GHz	37
Figure 26 - Position 1 - Smaller brick simulations - 5.15GHz.....	38
Figure 27 - Position 1 - Non-correlated Brick Size Simulation - 5.15GHz.....	39
Figure 28 - Position 1 - Smaller Brick Simulation - 5.35GHz	40
Figure 29 - Position 1 - Larger Brick Scenario - 5.35GHz.....	40
Figure 30 - Position 1 - Non-correlated Brick Size Simulation - 5.35GHz.....	41
Figure 31 - Measured Results for Position 2 - 5.15GHz	41
Figure 32 - Measured Result for Position 2 - 5.35GHz	42
Figure 33 - Position 2 – FDTD Dataset Simulation - 5.15GHz.....	42
Figure 34 - Position 2 – FDTD Dataset Simulation - 5.35GHz.....	43
Figure 35 - Position 2 - Larger Brick simulation - 5.15GHz.....	43
Figure 36 - Position 2 - Smaller Brick Simulation - 5.15GHz	44
Figure 37 - Position 2 - Smaller Brick Simulation - 5.35GHz	44
Figure 38 - Measured Result for Position 3 - 5.15GHz	45
Figure 39 - Position 3 - Small Brick Simulation - 5.15GHz.....	45
Figure 40 - Typical Reflection Coefficient Plot.....	47
Figure 41 - Reflection Coefficients and Frequency Dependence - 5GHz	47
Figure 42 - Reflection Coefficients and Frequency Dependence – 5.5GHz	48
Figure 43 - IPO3 execution and string input.....	49
Figure 44 - IPO_AoA execution and string input.....	50
Figure 45 - IPO_AoA execution end and final text file created	50

1) Introduction

In wireless communications, it is very important to know the characteristics of a wireless channel. Each individual link encounters different paths and obstructions, and is very important to formulate the exact loss from the transmitter to the receiver. Setting the receiver to a place with higher signal strength, and less fading, can enhance the performance and provide better quality of service. Especially in indoor environments where the structures are more complex, and various obstacles can cause degradation to the signal's quality, it is very important for the receiver to be placed in locations where the transmitter provides good coverage. A propagation model can predict and deduce the information needed to achieve such a high performing system. It will return the exact information required for the analysis, the evaluation and the implementation needed to improve the system's performance.

Geometrical Optics (GO), or Ray Optics, is an abstraction, which can be used to approximately model, how a ray propagates in the space [1]. It is constrained in its functionality as a ray when it is reflected or refracted by an object. On the other hand, Physical optics (PO), or Wave Optics as is also known, is a more comprehensive model, which includes wave effects such as diffraction, and interference, that cannot be accounted in GO [2]. Iterative Physical Optics (IPO) is a technique based on PO used to predict wave propagation [3]. Some of the main applications that IPO is used for, include the Radar Cross Section (RCS) of jet engine inlets or other flying objects and even some times of whole planets, the scattering effect in tunnels or open-ended cavities, implementations on Graphical Process Units (GPU) to improve the performance and indoor wave propagation which will be the main subject of study of this project [4].

The main idea underpinning this technique is that it uses the calculated current on the surface of an object to predict the radiation pattern. The process is executed iteratively and the current of each surface is updated every time. Compared with the precursors of IPO, it predicts more accurately the wave

propagation. One of the disadvantages of IPO is the high computational resources needed as part of the iterative process.

1.1) Aim

Many research works have focused in the implementation of IPO for tunnels or other open-ended cavities [3], [5]–[7]. This dissertation will focus on indoor wave propagation scenario and especially on a building consisting of 25 objects (walls, furniture, doors, etc.). The outcome of this project will be a simulator able to predict accurately the wave propagation for an indoor scenario, taking into account different factors as the frequency of the antennas, the position of the transmitter and the receiver, the different materials and objects that are situated inside a house, and the structure of the house, without the need of physical equipment and extravagant experiments.

1.2) Objectives

During this project, the conditions under which Ray Tracing (RT), Finite-Difference Time-Domain (FDTD), Shooting and Bouncing Ray (SBR) and Generalized Ray Expansion (GRE) give a valid approximation, and the conditions that IPO needs to be used will be identified. Looking at the theory of all the techniques, the advantages and disadvantages will be used to clarify the situations that they are suitable to be used. What is more, as the review of the literature will reveal works published in this field, the aim will be to exemplify the concepts of each techniques and will try to reinforce the conclusions reached from the theoretical study.

In order to extend the scope of the project even further, two programs built in Pascal from previous students of the University of Bristol (IPO_AoA and IPO3) [8], [9], will be used and expanded upon. The main goal of that is to implement the IPO technique in an indoor complex lossy environment. The results acquired from the new version of the software will be compared with existing results taken from measured experiments conducted from the Department of Electrical and Electronic Engineering at the University of Bristol. Some of the main objectives for this implementation are the following:

- Build a simulator that will implement IPO in various indoor environments and for different objects and materials.
- Implement some deficiencies found in the previous program (e.g. LOS link between the transmitter and the receiver)
- Attempt to overcome the drawbacks of the previous programs, (e.g. the calculation of the centre cell of a brick)
- Build an optimised code with the intention to keep the computation time and the need of resources as low as possible

This dissertation is separated in ten different sections. Firstly, there is an introduction, outlining the aims and objectives of the project, explaining the concepts that will be followed and the work that will be done during this dissertation. The background of RT, FDTD, SBR, GRE and IPO, and the advantages and disadvantages of these techniques will be given in section 2. An introduction to the software implemented will follow in section 3 and conclude in section 4 where the IPO algorithm will be discussed in correlation with the software functions. In section 5, the calculation of the field intensity at the receiver will be presented. The performance improvements will be explained in section 6 and the results will be discussed in section 7. A brief explanation of the software usage will be introduced in section 8, and a conclusion will summarize the main findings until now, identify question need to be addressed and explain the importance of this work. Finally, some proposals for improving the project further will be found in section 10.

2) Background

2.1) Ray Tracing (RT)

RT, which is based on GO, is the most popular and reliable method to model wave propagation in a specific site. As it is well known, modelling methods based on GO provide good results for electrically large objects [10].

For RT modelling, indoor environments are assumed to consist of homogeneous wall and structures. However, real world is not so ideal and more complex structures and inhomogeneous materials are used. Concrete cinderblock, reinforced concrete and dry-wall can be found in these structures, and are formed in an almost periodic occurrence [11]. Their transmission and reflection behaviour is very different compared to homogeneous walls and scattering field and cannot be predicted with RT.

Finally, an important factor that affects RT is the surface. When it is smooth, RT is accurate, but when it is coarse, this method is not so reliable because of the property of GO. In [12], a method to describe a surface as rough is presented and is calculated according to the height h . It is characterized by the wavelength λ and the angle of incidence ψ :

$$h = \frac{\lambda}{8 \sin \psi} \quad (1)$$

Characterizing a surface as coarse is based on the maximum distance difference between two paths and is respectively affected by the highest and lowest points found to clarify the distance difference between the two rays.

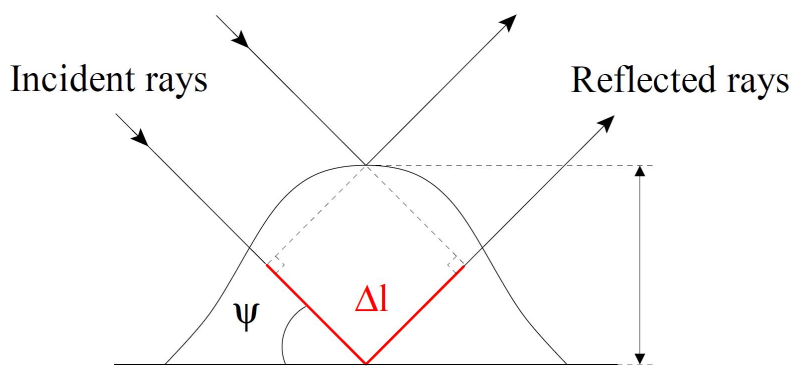


Figure 1 - Difference of Length Between two Paths Reflected by Roughness [12]

2.2) Finite-Difference Time-Domain (FDTD)

FDTD is another very well known method for indoor wave propagation. It is a numerical method based on Maxwell's equations [13]. The main idea behind FDTD is to directly solve the equations in time domain, because the changes of E-field in time are caused by the changes of H-field in space. Although, Maxwell's equations are continuous in the time and space domain, in FDTD method both time and space are discretized. Thus, the equations are converted into finite difference equations.

The results produced from this method are accurate, even for inhomogeneous and complex materials. What is more, it can capture the fast fading phenomenon successfully. Although it works accurately, and better than IPO, the disadvantage, is that it consumes a large amount of memory space to keep track of the data. In addition, a big amount of calculations is needed, even for small objects, so due to the computational requirements, it is very difficult to model a large object using FDTD.

2.3) Shooting and Bouncing Ray (SBR)

SBR is another technique for finding the electromagnetic field at an observation point due to a source. The ray's amplitude is approximated using the GO and the direction is calculated using Snell's Law and the Law of Reflection (LOR). The algorithm assumes that the internal scattering occurs on a sub-section of the surface. The reflected signal is found based on the approximation that this sub-section is part of an object that is practically infinite in extent, so that a single specular ray emerges to illuminate other portions of the target [14]. SBR is the fastest tracking technique from the ones that were mentioned before. Despite, the lack of accuracy of this method and the discontinuous predictions, including the limitations such as the cavity opening that needs to be large compared to the wavelength [14], make SBR a good choice when execution time is the first priority.

2.4) Generalized Ray Expansion (GRE)

In GRE, as in IPO, the incident field is replaced with the equivalent surface current which radiates later inside the structure that is modelled [15]. For a cavity scenario, while SBR technique tracks only the incident field which enters the cavity, GRE also includes the field diffracted inside the cavity by the edges at the open end. This method is applicable in arbitrarily shaped, non-planar open ends in a straightforward manner.

2.5) Introduction to Iterative Physical Optics (IPO)

IPO was proposed some years ago and was used to model the scattering effect in object cavities or tunnels [3]. The radiating pattern is calculated based on the given incident wave from the aperture of the cavity. IPO is formulated using the magnetic field integral equation (MFIE) [16] and is an iterative solution based on the current value of the surface of objects such as walls, furniture, etc. The solution is obtained after a number of iterations, which is closely related with the number of internal expected reflections. This value is achieved using Kirchhoff Approximation (KA).

2.5.1) Advantages and Disadvantages of IPO

Looking at previous works and comparing IPO with other modelling techniques, it is obvious that it has many advantages and achieves better performance. It can be implemented and work accurately in arbitrary shaped cavities [3] or complex building structures [10], something that is not applicable in RT due to the need of a simple geometry. What is more, rough surfaces [12], if handled by RT will give inaccurate results because beam radius cannot include the effect of small variations in surface because it is not small enough. On the other hand, IPO can handle quite well situations like these. In addition to that, SBR and GRE as every ray-based method, suffers from problems as caustics, ray divergence and the necessity of tracing a big number of rays through multiple bounces, thus lacks in accuracy compared to IPO [6].

A disadvantage of IPO is that it is highly demanding in computational resources, but needs lesser compared to RT and FDTD [3]. What is more, the need for

memory is more modest, because there is no need to store large matrices and the iteration method can execute faster if parallel programming and sectioning is used [5]. However, even though it is faster with lesser requirements, IPO is not convenient for everyday experiments based on complex environments without strong computational resources.

2.5.2) Kirchhoff Approximation (KA)

KA is one of the commonly used classical scattering models for rough surfaces, and is also known as tangent plane approximation. The basic idea of KA is that the surface fields at any point of a rough surface are approximated by applying a flat boundary plane tangent to the rough surface at that point [17]. In KA, the current value is related with the E- and H-field value of the surface and is used to convert the field value to the surface current value.

$$M_S = E_S \times \hat{n}_S \quad (2)$$

$$J_S = H_S \times \hat{n}_S \quad (3)$$

Using the previous equations, the magnetic and the electric current value can be calculated. M_S is the Magnetic surface current value, J_S is the Electric surface current value, \hat{n}_S is the normal vector of the surface, E_S and H_S are the field values of the surface.

2.5.3) Iterative Solution

The IPO method follows an iterative process to calculate the current values. At first, the E-field created from the transmitter, will introduce a current value on the surface of all the bricks that have LOS with the antenna. The updated magnetic current is based on the incident angle and the field intensity created by the transmitter. The affected bricks act as the new sources for the computation of the next order of surface current. During this step, and using the previously calculated values, the current on the bricks that have LOS with the first ones is calculated again and added to the previous values. In addition to that, the effect of the reflection of the transmitted rays is taken into account too. This step is repeated until a stable value of equivalent current is achieved (Fig. 2), (i.e. the change in the current is small enough to assume that it is stable and subsequent iteration can be neglected) [3]. The final step of the process is to calculate the

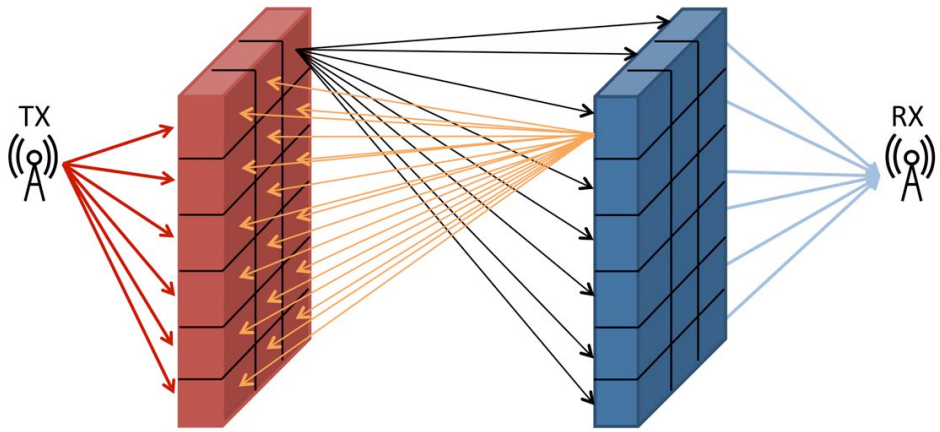


Figure 2 - Iterative Process of IPO algorithm

energy arriving at the receiver by calculating the field intensity coming from all the bricks that have LOS with the antenna. Later, a more detailed description of the process will be given in association with the simulator already implemented [9].

2.6) Building Material Properties

The building material properties that affect the radiation of the signal are the permittivity, the electrical conductivity and the thickness of the material. The permittivity of a material describes the resistance that is experienced when an electric field is formed inside a dielectric medium. The relative permittivity, or as is better known, the dielectric constant, is the ratio of the permittivity of a material, relatively to the permittivity of the vacuum which is equal to $\epsilon_0 = 8.854 \cdot 10^{-12} \text{ F/m}$ [1]. Relative permittivity is a dimensionless complex number. The real part is related to the stored energy within the medium and the imaginary part is related to the loss of the energy. , Permittivity can be affected by various factors such as humidity, temperature, position of the medium, frequency, etc.

The electrical conductivity describes the amount of current that flows inside a material and is reciprocal to the resistivity of that. It is denoted with the symbol σ and is measured in Siemens per meter (S/m). Materials with very low conductivity are classified as dielectrics, and a very low amount of current can flow inside the medium. Thus they can be used as insulators and create a high

signal attenuation [1]. Factors that affect the conductivity are the temperature, the skin depth, the porosity of the material, etc.

Finally, another important material property that affects the signal attenuation is the thickness of the object. The thicker the object, the more the loss will occur. These three properties will be taken into account for the different materials that will be used to calculate the propagation of the signal inside each object.

2.6) Introduction to Pascal

Continuing working on the previously implemented simulator from [9], Pascal programming language [18] will be used. It was developed in 1970, by Nicklaus Wirth and was named after the well known French-born mathematician and physicist, Blaise Pascal.

Pascal is a very easy to learn programming language and great for starters. Despite its simplicity, it can be used for advanced programming, due to its fast compilation and execution time and to the reduced memory requirements compared to other programming languages [19]. These features, combined with others that are very useful for advanced programmers (integration with assembly code, object oriented programming, compatible with other programming languages like C or Delphi, etc.), make Pascal a great choice for the implementation of the software [18].

Pascal language has a simple structure (Fig. 3). Each program starts with the **program** keyword and a list of external file descriptors as parameters. **Type** keyword is used to define other commonly used data types in terms of the predefined ones or define the length of a variable value. Under the **var** keyword, all the variables are declared. The main program is enclosed between **begin** and **end** keywords. Also **begin** and **end** keywords are used when a block of code bigger than one line is written inside a loop or a condition statement. Like all the structured programming languages, Pascal uses iterative statements with **while...do**, **repeat...until** and **for...to...do** loops, condition statements using **if...then...else** and **case...of**. Finally, functions can be written using the keyword **procedure** and can be called from another part of the program.

```

1 program ProgramName (FileList);
2
3 const
4   { * Constants Declaration * }
5
6 type
7   { * Types Declaration * }
8
9 var
10  { * Variables Declaration * }
11
12 procedure SubProgramName
13 begin
14   { * Function Implementation * }
15 end
16
17 begin
18   { * Main Program Implementation * }
19 end

```

Figure 3 - Simple Pascal Program Structure

Many compilers can be found online for Pascal language. To implement the software, Lazarus compiler and Free Pascal Lazarus IDE will be used [20]. Lazarus IDE (Fig. 4) is cross-platform software that is freely and widely used by the developers for Pascal programming. It can be used to create console and graphical applications, services / daemons and web applications.

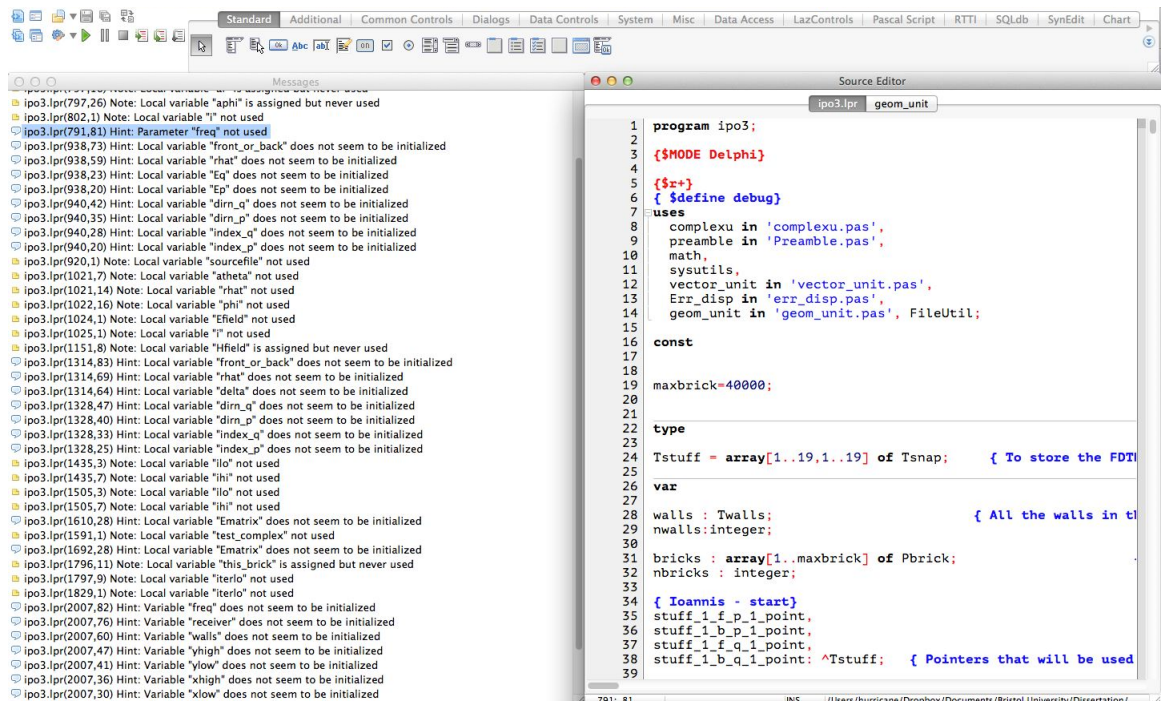


Figure 4 - Lazarus IDE Graphical User Interface

3) Introduction to the software

3.1) Introduction to IPO3 and IPO_AoA software

Two software applications are used to calculate the received energy. IPO3 is the application that implements the IPO algorithm and calculates the received field intensity. This program stores in files the surface current for each brick, caused by the transmitter. IPO_AoA, using as input these stored values, calculates the energy that arrives at the receiver as a function of the angle of arrival. The final output is a text file.

The basic input and output files for the software are the following. Both software use a string filename as an input that derives as a prefix for the following files. This prefix is represented later with “***”:

*****.source:** It contains the position and the frequency of the transmitter. The antenna used for the simulations, is a z-directed half-wave dipole.

*****.rx:** It contains the positions and the frequency of the receiver. Again, a z-directed half-wave dipole is used.

*****.wall:** These files are used to store the parameters for the walls. The structure of these files and some sample values are the following (the numbers in the file are given in scientific E-notation):

Lower left corner coordinates	Lengths in each direction	Wall Material	Vector in p direction	Vector in q direction	Vector in face direction
1.9 3.5 0	2.5 2.6 0.1	4	1 0 0	0 0 1	0 1 0
4.6 0 0	2 2 0.1	5	0 1 0	0 0 1	1 0 0
4.4 3.5 2.6	0.8 0 0.1	4	0 1 0	0 0 1	1 0 0

stuff.conf: Contains information on the data of brick scattering, the brick size and the number of cells and the data files that will be used. In detail, each line is described as follows:

Pathname for the scattering data files

Pathname for the empty data files

Pathname for the 1GHz data files

Pathname for the 5GHz data files

Number of the cells in the brick in the p direction

Number of the cells in the brick in the q direction

Ratio of number of cells in scattering data to number of cells used in IPO

Width of brick

Height of brick

Thickness of brick

Type of data files to be used: 1 – analytical, 2 – FDTD

brick.txt: It contains all the bricks that comprise the walls of the structure. It is used only for test purposes. Each line has the following structure:

centre of brick (x,y,z) centre of front surface (x,y,z) centre of back surface (x,y,z)

All the previous files are either input or output files for IPO3 software. The most important output files are the ones with “.prn” extension that are used to store the surface current for each brick of the walls. The name of these files depends on the number of the walls, the number of iterations of IPO algorithm and looks like *****_wall**_*_.prn**. The format of these files is:

*x y z px py pz qx qy qz nx ny nz Re(Jp1) Im(Jp1) Re(Jq1) Im(Jq1) Re(Jp2) Im(Jp2)
Re(Jq2) Im(Jq2)*

where (x,y,z) are the coordinates of the centre of the brick, (px,py,pz) is the vector of the “p” direction, (qx,qy,qz) is the vector of the “q” direction, $Jp1$ is the “p” component of the current density on the front face, $Jp2$ is the “p” component of the current density on the back face. Similarly for $Jq1$ and $Jq2$.

A special version of the .prn files, is the *****_source_to_receiver.prn**, which contains the coordinates of the centre of the transmitter and the complex field intensity that is created from the LOS link between the transmitter and the receiver.

These .prn files are used by the IPO_AoA software to calculate the received energy. The output is a text file (*****.txt**) that contains a snapshot of numbers corresponding to the azimuth and elevation angles. The structure of this file is the following:

Azimuth angle, Elevation angle, horizontal magnitude, horizontal dB, vertical magnitude, vertical dB, brick number, wall number, brick centre

The last columns are mainly used for debug and test purposes only. The first three columns are plotted using a simple program implemented in Matlab in a 2-D style plot and this is the final result from the simulation.

3.2) Structures

For the implementation of the simulator, three key structures were used. These structures are the:

- Wall
- Brick
- Cell

Wall and brick structures are abstract because they point in different objects and periodic parts of these objects respectively.

3.2.1) Wall

As a “wall” is called, each object or wall that is found in the complex structure used for the simulations. Each object has two different coordinates, the higher and the lower (Fig. 5), defined in the Cartesian coordinate system that specify the size of the wall in space. The lower coordinate that depicts the lower left corner of the face of the wall is given in the “***.wall” file. The upper right coordinate of the back of the wall is calculated in IPO3 using the length in each direction and the thickness values in the same file.

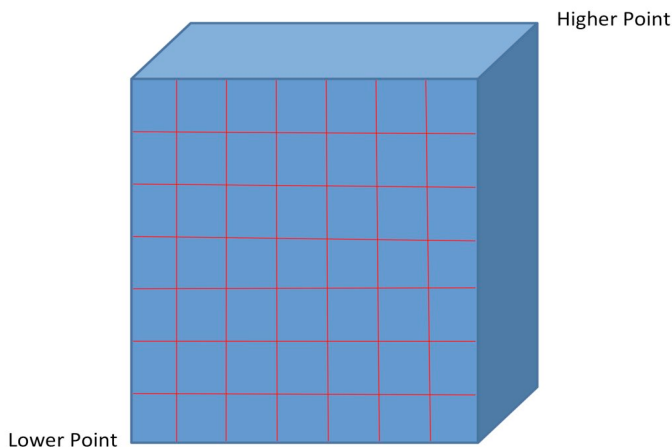


Figure 5 – Lower and Higher Coordinates

The direction vectors of the wall are expressed in the (P, Q, Face) system (Fig. 6). The face vector is the normal vector of the wall. The P and Q vectors point at the tangential axis in the surface. The reason of using this system is that the wall may face in any possible direction that is pointed with the face vector. What is more, these vectors are used to determine the front or the back surface of the wall and the incident angle.

3.2.2) Brick

The brick structure uses the same direction vectors as the wall before (Fig. 7). The values are inherited from the wall that each brick belongs to. The wall is indicated with the *wallID* in the structure. Each brick has three different coordinates. “Centre” is the coordinates for the centre point of the brick. “Front” and “Back” declare the centre point of the front and the back surface respectively and are calculated using the “Centre” coordinates and the thickness of the brick. A vector called “LOS” is used to determine the bricks that have LOS with each specific brick. A flag is raised in the Nth position of the vector if the LOS conditions are met, pointing that there is not an object intercepting between the two bricks. Finally, the E-field values for both the front and the back surface of the brick are stored in the *fvalue* and the *bvalue* matrices. Some more matrices (*fvalue*, *bvalue*, *ftvalue* and *btvalue*) are used for the IPO calculations. All the *F* and *B* values are set to zero at the beginning and are updated from the IPO algorithm.

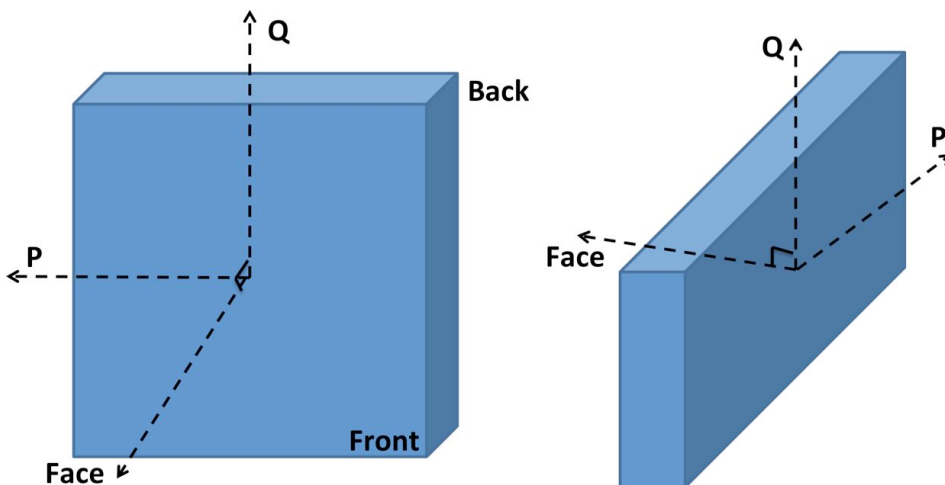


Figure 6 - (P, Q, Face) Coordinates and Front/Back Surfaces

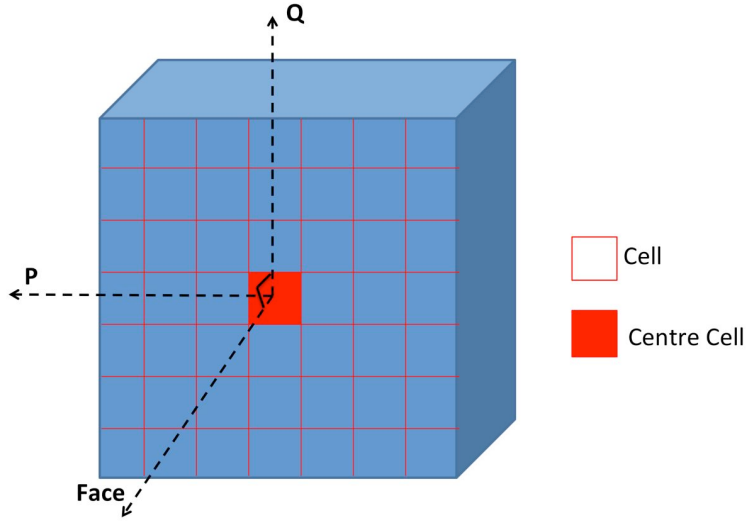


Figure 7 - Brick Coordinate System, Cells and Centre Cell of the Structure

3.2.3) Cell

Finally, the cell height and width are determined from the configuration file given as an input. The most important cell is the centre one that is used for calculating the received energy. More information about the cell structure will be given later.

3.3) Geometry

All the objects are loaded from the input file with “.wall” extension. This file needs to be created using “*geoff_wall.pas*” application, before conducting a simulation. The inputs for this program are the lower left corner of the wall, the lengths in each direction, the thickness and the object type. In the field “*wall material*,” the five different sub-categories for an object are clarified as following:

1. External Wall
2. Internal Wall
3. Door
4. Stairs
5. Furniture

These five objects will be used later, in order to characterize the material that makes up an object. All the wall structures consist of a specific number of bricks. The number of bricks is calculated depending on the width and the height that can be found in “*stuff.conf*” file. These values are given in meters and are used to

calculate the number of bricks in each direction. The length of the wall is assumed as an exact multiply of the brick size and the bricks are being square shaped.

Finally, the number of cells is given again in the “*stuff.conf*” file. Given the number of cells in each direction, the values of the total number of cells, the cell size and the cell area can be calculated.

3.4) Scattering Results for Different Materials

A house or a building in general, is composed of many different objects. Each object due to the different dielectric properties of the materials consisting it, will radiate, reflect, or diffract a ray with a different way. During this project’s simulations, where a two floor house was used, in order to get more accurate results but keep the complexity and the computational resources required as low as possible, it was assumed that the house is composed of the five different objects that were mentioned before.

To speed up the computation time, the radiation inside the objects is precomputed, stored, and loaded in the simulator when needed. This is feasible due to the periodicity of the bricks inside each wall. Although this increases the memory needed, today’s PCs are capable of covering these memory requirements. This leads to drastically decreasing the execution time.

Two different kinds of datasets will be created, regarding the number of objects that will be used in each simulation and the method that the scattering data were calculated. These two methods calculate the radiation effect for a single brick, regarding the angle of the incident ray divided in the azimuth and the elevation angle [8].

3.4.1) FDTD Simulation

The first method that was used is the FDTD method. FDTD method was introduced in [21] to discrete the structure material in unit bricks and to calculate and save the scattering data. These results were used in IPO3 and

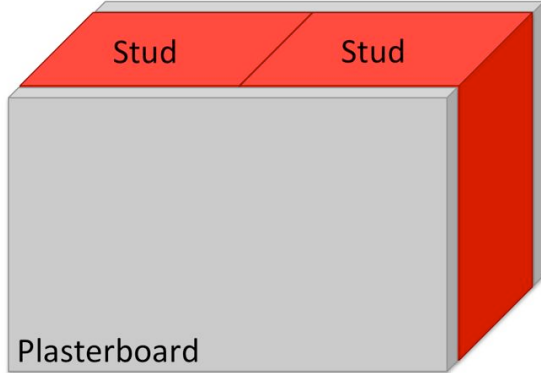


Figure 8 - FDTD Simulation Geometry of a Single Brick

IPO_AoA software implementation [9] and will be used during this dissertation too.

The FDTD method simulate parallel and perpendicular polarized plane waves arriving at various angles [8]. For these simulations, it was assumed that all the objects in the house are composed of two plasterboards and two studs between them (Fig. 8), with the following material properties (Table 1):

Material	Permittivity	Conductivity	Thickness
Plasterboard	2.21	0	0.125
Stud	3	0.2	0.055

Table 1 - FDTD method's Material Properties

3.4.2) Analytical Simulation

The analytical method is the second method used to calculate and store the scattering data for all the objects mentioned above. The input parameters of the software (*slab3*) are the permittivity, the conductivity, the thickness, the frequency and the brick size. The brick size used in *slab3* application, is correlated with the brick size used in the simulations later. This software is used to derive the phase gradient across the brick, which is not known in IPO algorithm simulator. Therefore, the two sizes should be the same. This software can be used for objects composed of layers of different materials as well, by specifying the previous parameters for each layer's material and the number of layers. The input of *slab3* program is a file with the following structure:

*brick width, brick height
number of layers, frequency
permittivity, conductivity, thickness (one line per different layered material)*

At first, the materials that consist each object had to be specified, in order to choose the proper values for all the material properties. One of the problems that needed to be addressed was the nihility of knowledge for the materials used to build the building. Thus, some assumptions need to be made. From [22], [23] and [24] a typical design of an external wall was derived. Therefore, it was assumed that the External Wall is composed of five layers of materials. From the outer to the inner side of the wall, the materials used are the following (in the brackets, the thickness of each layer can be found):

- 1) Plaster (0.01 m)
- 2) Facade Brick (0.125 m)
- 3) Cavity Insulation - Air (0.1 m)
- 4) Red Brick (0.105 m)
- 5) Plaster (0.01 m)

For the other objects, homogeneous materials were chosen to represent the object because the other layered materials (plaster, paint, leather etc.) affect negligibly the radiation because they are very thin:

- Door - Wooden Door (0.04 m)
- Internal Wall - Red Brick (0.105 m)
- Stairs - Wooden Board (0.03 m)
- Furniture - Wooden Board (0.05 m)

Before calculating the scattering results, all the electrical properties' values were collected. For the chosen materials and for the specific frequencies that the simulations will take place, the literature and the research results so far do not provide accurate values for all the electrical properties. The problem is mostly with the values of the permittivity that is dependent with the frequency. In [25], it can be seen that regarding the material, the relative permittivity may be proportional, inversely proportional or following a wandering pattern. As a rule of thumb, the relative permittivity for all the isotropic materials, can be considered as inversely proportional to the frequency. Thus, the permittivity

values found in the literature will be used for a specific frequency (5.15GHz) and all the others will be approximated using the previous rule. The only material that does not follow this rule is plaster, for which the relative permittivity is proportional to the frequency [25]. All the electrical properties are summarized in Tables 1 and 2.

A great advantage of the analytical method is the time needed for the simulations to be conducted. Each material's simulations needs about one minute to be executed. This execution time is really short compared to the FDTD method that needs some days to calculate the scattering data for a single brick. Therefore, the analytical method was the only one chosen to simulate the different objects and materials in the expense of accuracy of course that may have been achieved with FDTD method.

Material	Permittivity	Conductivity	Thickness
Doors [25]	5.84	0.06	0.04
Red Brick (Int. Wall) [25]	3.58	0.11	0.105
Stairs (Wooden Board) [26]	2	0.06	0.03
Furniture (Wooden Board) [26]	2.2	0.06	0.05
Ext. Wall (5-layer Materials)			
Plaster [27]	2.02	0.014	0.01
Facade Brick [28]	4.6	0.051	0.125
Cavity Insulation (Air)	1	0	0.1
Red brick (inner wall) [25]	3.58	0.11	0.105
Plaster [27]	2.02	0.014	0.01

Table 2 - Building Material Properties for 5.15GHz.

Material	Permittivity	Conductivity	Thickness
Doors	5.62	0.06	0.04
Red Brick (Int. Wall)	3.45	0.11	0.105
Stairs (Wooden Board)	1.93	0.06	0.03
Furniture (Wooden Board)	2.11	0.06	0.05
Ext. Wall (5-layer Materials)			
Plaster	2.1	0.014	0.01
Facade Brick	4.43	0.051	0.125
Cavity Insulation	1	0	0.1
Red brick (inner wall)	3.45	0.11	0.105
Plaster	2.1	0.014	0.01

Table 3 - Building Material Properties for 5.35GHz.

At the beginning of the IPO simulation, and depending on the type of the data files that is chosen, either the analytical or the FDTD scattering dataset is loaded. In order to choose the appropriate dataset each time, the datasets are stored under a specific folder, which is stated as the path of the scattering data files in the *stuff.conf* file. The dataset for each frequency is stored in different subfolders. For the analytical datasets, another layer of subfolders is used to store the scattering data for each material. Regarding the frequency of the receiver and the transmitter, this frequency subfolder's name, combined with the path of the scattering data files creates the pathway that the dataset will be located.

To keep the simulator dynamically implemented, pointer variables were used to point at the specific material's scattering dataset each time. Later in the report, it will be explained how these scattering data are used to calculate the brick's surface current.

4) Iterative Physical Optics Algorithm

4.1) Line of Sight Relationship

LOS relationship is very important for the implementation of IPO algorithm. The same mechanism is used to determine if there is LOS between two brick or the walls or between the transmitter and the receiver.

To achieve LOS between two different objects, no walls should intersect between these objects. The algorithm of LOS runs for all the possible combinations of bricks. At first, the LOS value is set to 1, indicating LOS relationship between the two selected bricks. The first condition that is checked is if the two bricks are part of the same wall. If this is met, then LOS value is set as false and the next pair of bricks is chosen. If not, the program will take the rest of the bricks and decide for each one of them. “*pidtot*” is a counter that is used in this function. The algorithm keeps running while the wall chosen is not the same wall of the two bricks that are compared and while “*pidtot*” is equal to zero. If the counter is increased, then an object intersects between the two bricks and there is no LOS. The judgement of LOS between two bricks is based on solid geometry.

4.1.1) Solid Geometry

The first step to judge about the LOS between two bricks is the calculation of the distance between them and the comparison with the distance of a wall. The first situation that there is LOS between two bricks is when the distance between them is shorter than the distance between the brick and a specific wall (Fig. 9).

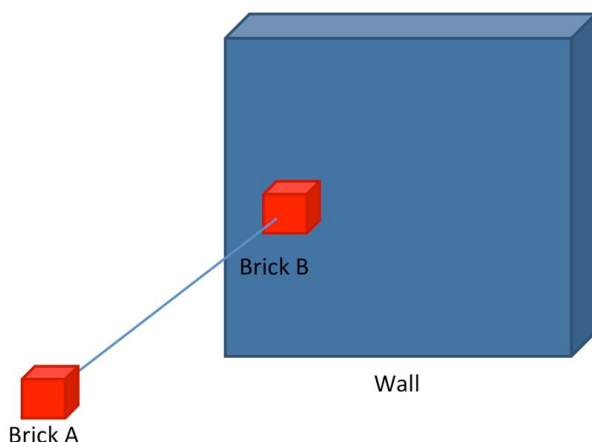


Figure 9 – First LOS situation – Brick-Brick Dist. shorter than Brick-Wall Dist.

When the distance is longer compared to the distance of the brick to the wall, then those bricks are not on the same side of the wall. In that case, no walls intersect between these two bricks, and then another situation with LOS is found (Fig. 10). On the other hand, if a wall intersects between these two bricks, NLOS exists (Fig. 11).

To find an intersection point between the straight line of the two bricks and the wall, the coordinates of the six surfaces of the wall and the centres of the bricks are checked using the line equation in space:

$$\frac{x - x_1}{x_2 - x_1} = \frac{y - y_1}{y_2 - y_1} = \frac{z - z_1}{z_2 - z_1} \quad (4)$$

If none of the surfaces intersects with the straight line between the two bricks, the LOS is not blocked between them.

4.2) Initialisation of LOS

Before the IPO algorithm, all the bricks will update their “los” vector and the existence of LOS link between the transmitter and the receiver will be found. This information is used from the IPO algorithm, and for a chosen brick, the bricks that are affected are the ones that have LOS with it.

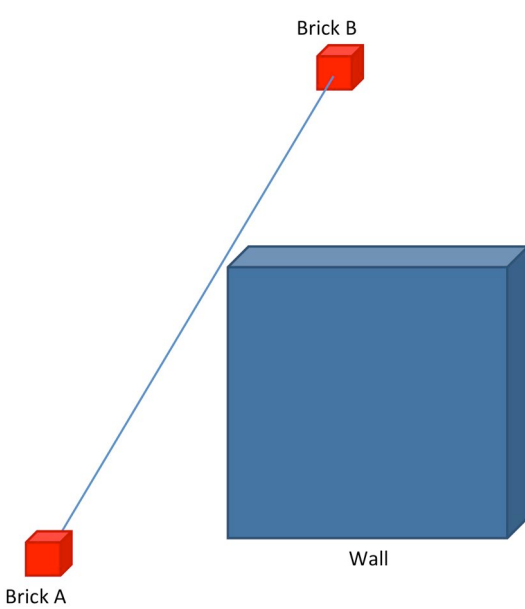


**Figure 10 – 2nd LOS situation – Brick-Brick Dist.
Longer than Brick-Wall Dist.**

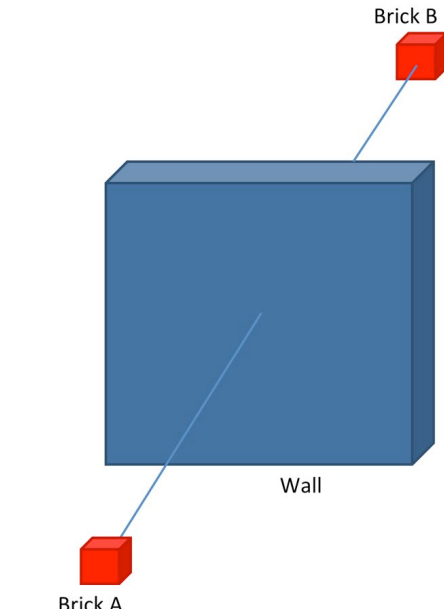


**Figure 11 - NLOS Situation – Wall intersects
between bricks**

4.3) E-field from source to receiver

When LOS exists between the two antennas then a very high intensity signal is received that will contribute significantly at the total received energy. For a very thin dipole, E- and H-field closed form equations can be obtained in all the regions. But, in most cases, like in this project, far-field is only used due to the complications of the integration of the vector potential A. What is more, for a frequency of about 5GHz, the wavelength is about 6cm and is very short compared to the distance between two objects inside a house. In [29], the E-field equation for a z-directed finite dipole antenna in the far-field is given as:

$$E_\theta = j\eta \frac{I_0 e^{-jkr}}{2\pi r} \left[\frac{\cos\left(\frac{kl}{2}\cos\theta\right) - \cos\left(\frac{kl}{2}\right)}{\sin\theta} \right] \quad (5)$$

where r is the distance between the two antennas, k is the wavenumber (Eq. 8), l is the length of the dipole antenna, θ is the elevation angle, I_0 is the antenna current (Eq. 7) and η is the intrinsic impedance (Eq. 6).

$$\eta = \sqrt{\mu_0/\epsilon_0} \quad (6)$$

$$I_0 = V/R \quad (7)$$

$$k = 2\pi f/c \quad (8)$$

For the previous equations, c is the speed of light, f is the frequency, V is the potential difference across the antenna, R is the resistance of the antenna, μ_0 is the magnetic constant and is equal to $\mu_0 = 4\pi 10^{-7} \text{ Nm}^{-1}$, ϵ_0 is the vacuum permittivity, is equal to $\epsilon_0 = 8.854 * 10^{-12} \text{ F/m}$ and can be calculated as:

$$\epsilon_0 = 1/\mu_0 c^2 \quad (9)$$

During the simulations, half-wavelength dipole were used as transmitter and receiver antennas. Half-wavelength means that $l = \lambda/2$. The input impedance for a half-wavelength dipole is equal to $Z_{in} = 73 + j42.5 \text{ Ohms}$. By reducing slightly the length of the dipole to 0.48λ , the input impedance becomes $Z_{in} = 70 \text{ Ohms}$, and there is no reactive component. This will decrease the calculation complexity with the radiation pattern remaining virtually the same [30]. Using all the above

and a potential equal to $V = 1$ Volt, the antenna's current is equal to $I_0 = 1/70$ A and the E-field equation is the following [29]:

$$E_\theta = j\eta \frac{1/70 e^{-jkr}}{2\pi r} \left[\frac{\cos\left(\frac{\pi}{2}\cos\theta\right)}{\sin\theta} \right] \quad (10)$$

To implement this equation, at first the existence of a LOS link between the transmitter and the receiver is checked. The transmitter and the receiver for the purposes of the simulator are implemented as two special bricks and are dimensionless. They are represented as a point in the space and their coordinates is given in the files `***.rx` and `***.source`. E-field values are initialized as zero. When LOS exists between the two antennas, the distance and the elevation angle between the antennas are calculated. Later using the Eq. (10) the E-field is calculated and is returned to the main program, where it is stored in the `***_source_to_receiver.prn` file. If there in no LOS between the two antennas, then zero is returned.

4.4) Radiation pattern from the transmitter to the bricks

Before starting iterating around the IPO algorithm, the effect of the transmitter to the first set of bricks needs to be calculated. The function starts again by checking which bricks have LOS with the transmitter using the “LOS” vector that was updated before. For all the bricks that have LOS, the distance and the elevation angle from the transmitter is calculated. Later, using the Eq. (10) the E-field is found. The incident field at the centre of the brick is divided in two components P and Q, which are the two tangential polarized fields of the incident wave and are tangential with the surface of the brick.

In order to calculate the surface current of the bricks, the incident angle needs to be calculated first. The incident angle (Fig. 12), is a combination of the azimuth and the elevation angle and is used to pick the correct file of the FDTD or the analytical scattering results. The incident angle can be found using the \hat{r} vector in the direction of the ray and the P and Q components with Eq. (11) and (12).

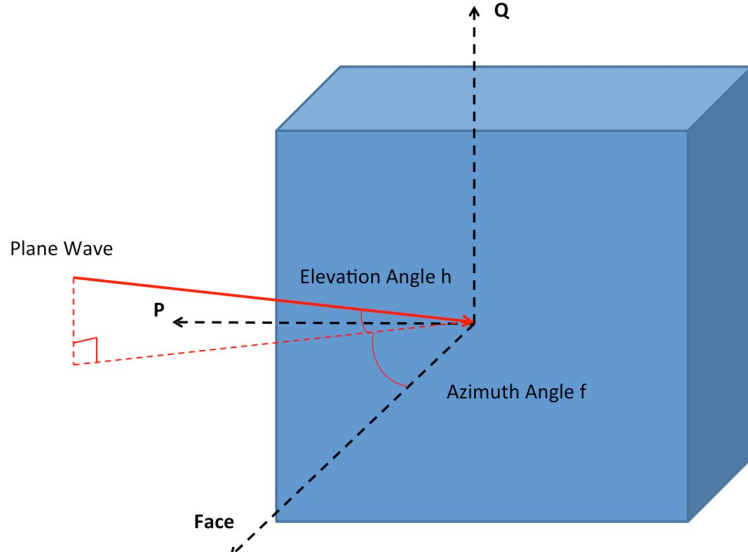


Figure 12 - Incident Angle

$$\theta = \cos^{-1}(\hat{r}\vec{Q}) \quad (11)$$

$$\varphi = \cos^{-1}(\hat{r}\vec{P}) \quad (12)$$

Both the analytical and the FDTD datasets are calculated for specified angles as it was mentioned before. Thus, after the incident angle is calculated, the nearest simulated angles are picked up and correlated with the results from the analytical or the FDTD simulations.

Additionaly, the decision concerning the facing of the target brick is done using the distance to the centre of the front and the back surface. Knowing the incident angle and the tangential polarized fields, the incident field in that polarization direction is multiplied by the scattering values from the FDTD or the analytical simulations. The two multiplied results are added together and give the updated surface current value for the receiver brick. Finally, these values are stored in the “fvalue” and “bvalue” variables and are used when each brick acts as a transmitter.

4.5) Radiation from brick to brick

The radiation exerted on the bricks with LOS with the transmitter, causes the creation of a surface current on these bricks. In addition to that, this current causes these bricks to act as transmitter to all the bricks that have LOS with them. The first step for this procedure is to calculate the angle between the

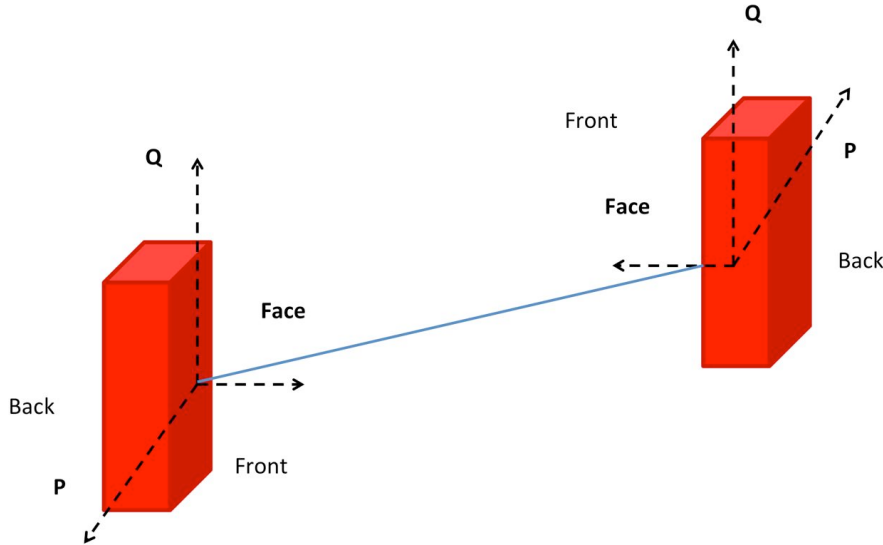


Figure 13 - Two bricks' front surfaces facing each other

source and the receiver brick and to ascertain whether the ray is between the front or the back surface of the bricks (Fig. 13). The four possible combinations for the brick surfaces that have LOS are as follows:

1. Front surface of source brick → Front surface of receiver brick
2. Front surface of source brick → Back surface of receiver brick
3. Back surface of source brick → Front surface of receiver brick
4. Back surface of source brick → Back surface of receiver brick

The coordinates of each side's centre are used to calculate the distance between all the previously mentioned combinations. The shorter distance implies the starting and the ending point of the ray and the facing geometry of the two bricks. Using the shortest distance's value, the \hat{r} vector is found and it is analysed in the P and Q components in order to calculate the azimuth angle φ and the elevation angle θ as previously.

Using the E-field value and the scattering data, the equivalent current value is calculated on the source brick using the Kirchhoff approximation (Eq. 2 and 3). The next step is to rotate the current values in the global (x, y, z) coordinate system. Later, the electric and magnetic potential vectors \vec{F} and \vec{A} , are used to calculate the radiation field:

$$\vec{F} = \frac{\epsilon}{4\pi} \iint_S \frac{\vec{M}_s e^{-jk|\vec{r}-\vec{r}'|}}{|\vec{r}-\vec{r}'|} ds \quad (13)$$

$$\vec{A} = \frac{\mu}{4\pi} \iint_S \frac{\vec{J}_s e^{-jk|\vec{r}-\vec{r}'|}}{|\vec{r}-\vec{r}'|} ds \quad (14)$$

where S is the surface area of the brick, \vec{r}' is the position of the surface current, and \vec{r} is the position of another brick or the receiver. The E and H fields are calculated later by the following equations:

$$E_A = -j\omega A - j \frac{1}{\omega\mu\epsilon} \nabla(\nabla \cdot A) \quad (15)$$

$$H_F = -j\omega F - j \frac{1}{\omega\mu\epsilon} \nabla(\nabla \cdot F) \quad (16)$$

Because the receiver is in the far field, only the tangential components E_θ and E_ϕ are required since $E_r \approx 0$.

Knowing the incident field values, the angle of the impinging ray relatively to the P and Q components is calculated later, as before. Regarding the facing of the target brick (*front* or *back*) and using the correspondent scattering data the induced field values are calculated and added to the total value (*fvalue* and *bvalue*). Finally, all the field values are stored in the “***.wall” files to calculate the received energy later.

5) Received Signal (Final Step of IPO algorithm)

From the data that were previously stored in the “***.wall” files, the received energy can be calculated. As before, the receiver will be affected just from the bricks that have LOS with the antenna. To calculate the effect and thus find the received energy, for all the combinations between an elevation and an azimuth angle, the targeting brick at that direction needs to be found and the fields coming from that brick will be calculated. The range of the elevation angle is between -90° and 90° and the range of the azimuth angle is between -180° and 180°.

At first, the configuration for the walls, the size of the bricks and the coordinates for the receiver and the transmitter are loaded in the software. The centre cell (Fig. 7) of each face of the brick is very important because it can be used for representing the average surface field intensity for the brick. The centre cell is calculated using the next equation and is rounding to the nearest integer:

$$\text{Centre Cell} = \text{cells in columns} * \left(\frac{\text{cells in rows}}{2} \right) + \left(\frac{\text{cells in columns}}{2} \right) \quad (17)$$

5.1) Bricks Contributing to the Received Energy Calculation

The brick that contributes to the received energy for a combination of an azimuth and an elevation angle, is called the target brick (Fig. 14). All bricks will be checked against the conditions for being the target brick for the specific azimuth and elevation angle. These angles will be converted to the angle related to the (x, y, z) coordinate system using the three-cosine theorem.

$$\cos z = \cos(90 - \varphi) \quad (18)$$

$$\cos x = \cos \varphi \sin(90 - \theta) \quad (19)$$

$$\cos y = \cos(90 - \varphi) \cos(90 - \theta) \quad (20)$$

With the coordinates of the receiver's centre and the angle, the line function can be expressed as:

$$\frac{x' - x}{\cos x} = \frac{y' - y}{\cos y} = \frac{z' - z}{\cos z} \quad (21)$$

where (x, y, z) are the coordinates of the receiver's position, (x', y', z') are the coordinates of a point on this line and $\cos x, \cos y, \cos z$ are the cosine values to the x, y and z direction respectively. In addition to that, the higher and the lower points of the bricks need to be calculated before finding the target brick.

$$\text{Higher Point} = \text{center} + (\text{height} * \vec{P} + \text{width} * \vec{Q} + \text{thickness} * \vec{Face}) * 0.5 \quad (22)$$

$$\text{Lower Point} = \text{center} - (\text{height} * \vec{P} + \text{width} * \vec{Q} + \text{thickness} * \vec{Face}) * 0.5 \quad (23)$$

For the condition of the target brick to be met, all the faces of the brick are checked using the solid geometry that was introduced before and if an intersection point is found, then this is the target brick. The higher and lower points will be used to calculate the whole surface that a face of the brick covers, and if the intersection point is inside the boundaries of this surface then this brick is indicated as the target brick.

When $\cos x = 0$, there are either none or infinite intersection points because the line function is parallel to the brick surface. None of these situations fits the condition of finding the target brick.

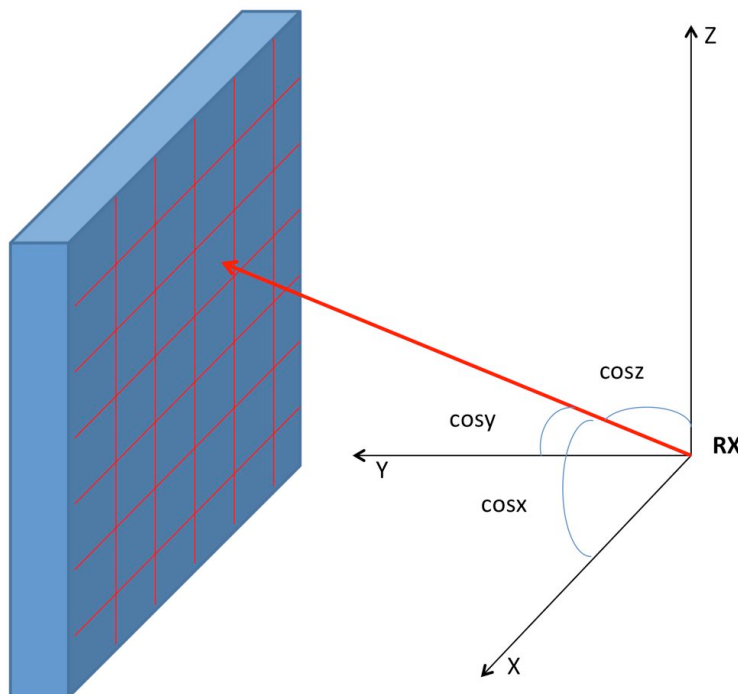


Figure 14 - Target Brick - Three Cosine Theorem

For all the bricks that meet the previous condition, the distance from the receiver is calculated. Finally, the brick with the shortest distance is declared as the target brick and the incident field of that is calculated.

5.2) Field Intensity and Total Received Energy

When the target brick is found, the E-field from this brick to the receiver is calculated. Using the same procedure as the radiation between two bricks, the currents on each cell are calculated (Eq. 2 and 3). Later the potential vectors (Eq. 13 and 14) are used to calculate the intensity field on the target brick (Eq. 15 and 16). The magnitude of the energy in the receiver is calculated by squaring the value of the field intensity:

$$\text{Energy in the Receiver} = \sqrt{\text{field intensity}.re^2 + \text{field intensity}.im^2} \quad (24)$$

The results of this software are stored in a “***.txt” file with the same name as the input parameter. In addition to that, the E-field from the transmitter is also considered and added to the file. The result is plotted in a 2-D plot using a program implemented in Matlab. In Fig. 15, a summary of IPO’s algorithm can be seen in terms of the application that is implemented.

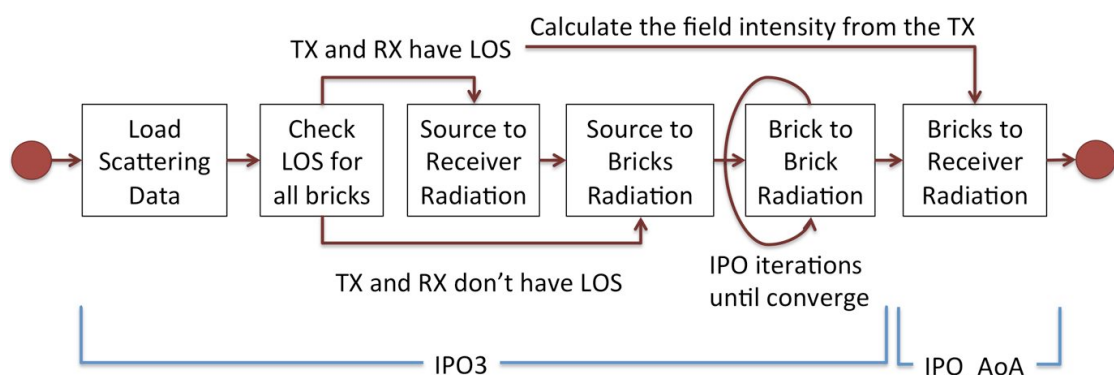


Figure 15 - IPO Algorithm and Software Applications Implementing it

6) Performance Improvement

6.1) Code Optimisation

The previous version of the software needed more than 10 hours for a single simulation. Thus, it was necessary for the code to be optimised in order to be able to run faster and give the opportunity for more complex structures to be simulated.

In order to improve the performance, optimisation switches were used and especially the highest level of optimisation from Lazarus IDE. This was the Level 3 Optimisation switch (-o3). Some of the improvements that it introduces are re-ordering the function declaration, deletion of never used function, etc. The most important improvement of -o3 is the introduction of software pipelining which has the advantage of running more iterations in parallel using unrolling and single instruction multiple data (SIMD). Thus, many “No Operations” (NOPs) in the code are filled with instructions taken from other iterations which speedup the calculations [18].

What is more, smart linking improves the performance of the software. When a program is smart-linked the compiler will only link in the code that is actually needed and leave out the rest. This leads to a smaller binary, which loads faster and speeds up the execution [20].

Finally, removing debugging information from the executable file will improve the execution time. Although, this has the drawback that programming bugs may be harder to be located and removed. Therefore, this is the last improvement introduced, once the program is proven to run smoothly.

6.2) Software Convergence

In IPO algorithm, the number of iterations represents the number of important reflections needed for the simulation to converge [3]. Execution time increases linearly to the number of iterations, thus iterations that negligibly change the final result can be prevented. Therefore, to improve the performance further, a

convergence rule was introduced in the simulator. In [3], it was proven that 3 iterations are enough for a tunnel structure. For a more complex structure as a building more iterations will be needed. The maximum hardcoded number of iterations for the IPO algorithm was set to 19.

A temporary counter, a value that represents the convergence, and 60 brick field intensity values are used, to test the convergence of the algorithm. In order to check it, the next equation for the complex distance of two numbers is used:

$$Distance = \sqrt{(Old\ field\ value.re - New.re)^2 + (Old.\ im - New.\ im)^2} \quad (25)$$

Distance = 0.01 is used as a threshold value. After experimentation with different values, this value was proven as the one that the results' plots almost overlay the results of the previous iteration (Fig. 16). When the distance between the two field values is bigger than the threshold, the counter is increased because the IPO algorithm is not yet converged. After looping the 60 values, and in the case that the counter is equal to zero, the algorithm is converged and the convergence variable is increased by one. On the other case, this variable is initialized as zero again. When none of the values increasing the counter is bigger than the threshold for three iteration in a row, then the algorithm is assumed to be converged and the execution ends.

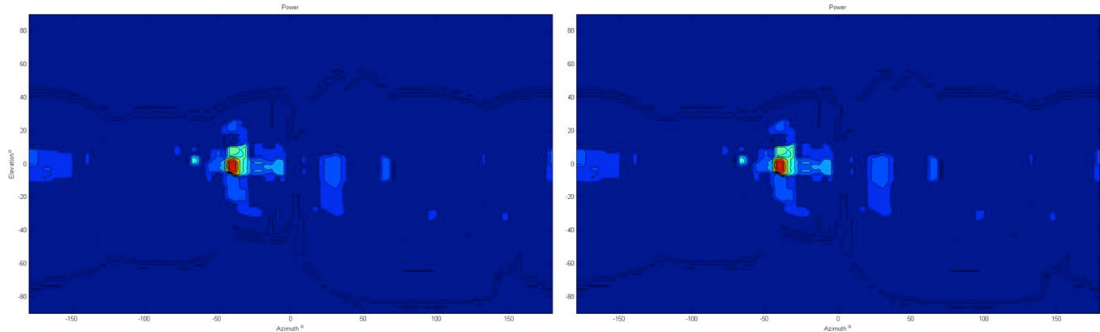


Figure 16 - Results Plotted from Two Different Iterations that Overlay

7) Results

Various simulations were conducted by taking into account different parameters that may affect the radiation pattern and the received energy. The different configurations used, are a combinations of the following cases:

- Different positions for the receiver.
- Different frequencies (5.15GHz, 5.35GHz).
- Different number of cells (100 (10x10) per brick, 400 (20x20) per brick).
- Different brick sizes (0.1m for width/height, 0.2m for width/height).
- Different Scattering dataset chosen for the simulation.

The house that was used for the simulations, consists of 25 different objects. A graphical representation of this house is created in Matlab (Fig. 17).

The measured and the simulated results are plotted using a simple Matlab program. The simulated ones are the outcome from the IPO_AoA program. The results represent all the combinations of azimuth and elevation angles around the receiver and the warmth of the colour describes the energy at that specific combination of angles arriving at the antenna.

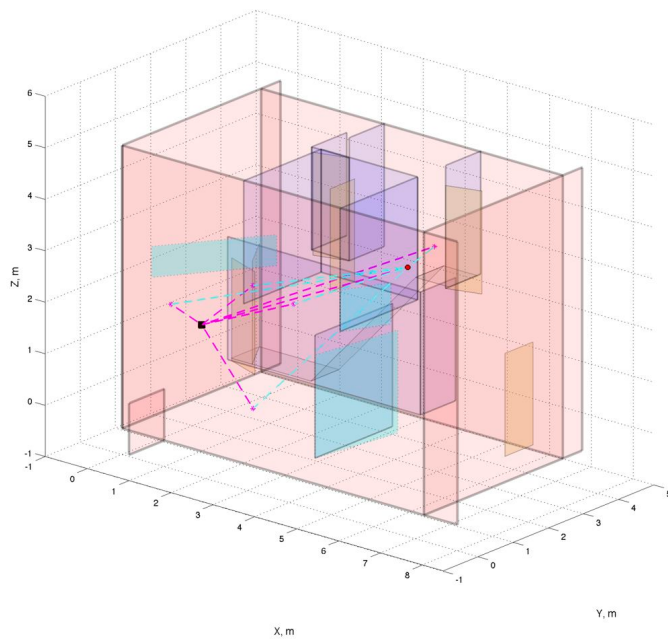


Figure 17 - House Layout

7.1) LOS Link

The LOS link was tested at first (Fig. 18 and 19). The receiver was placed at the same position for both frequencies. Unfortunately, the measured results that were provided did not include a scenario with a LOS link between the transmitter and the receiver, thus a comparison with measured results is not feasible. The simulator was tested using both FDTD and analytical dataset and the results were identical for both methods.

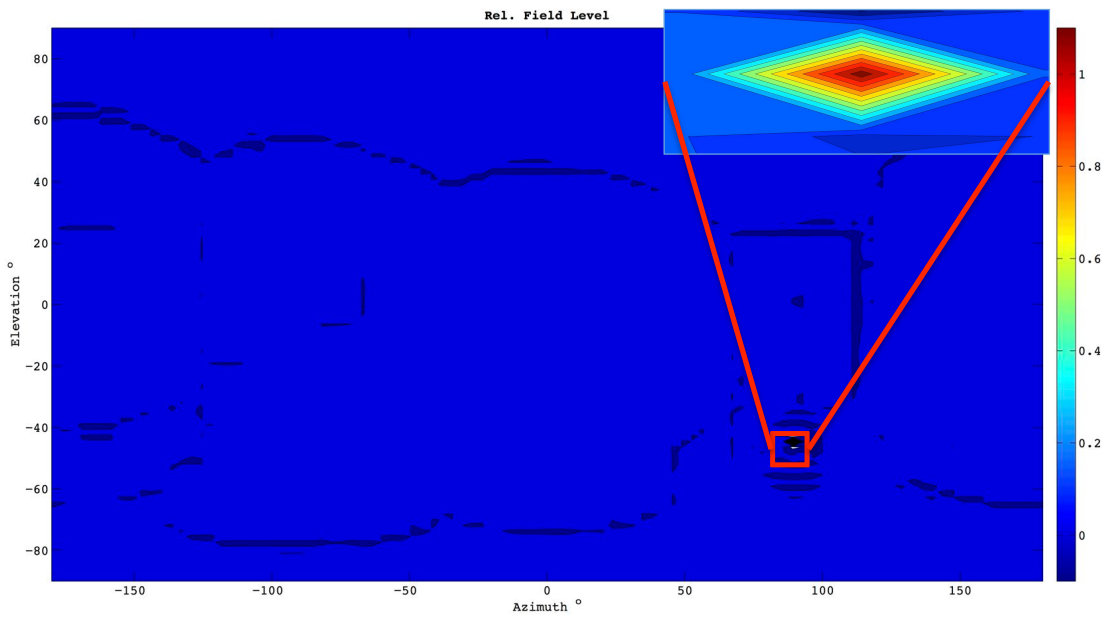


Figure 18 - LOS link for 5.15GHz

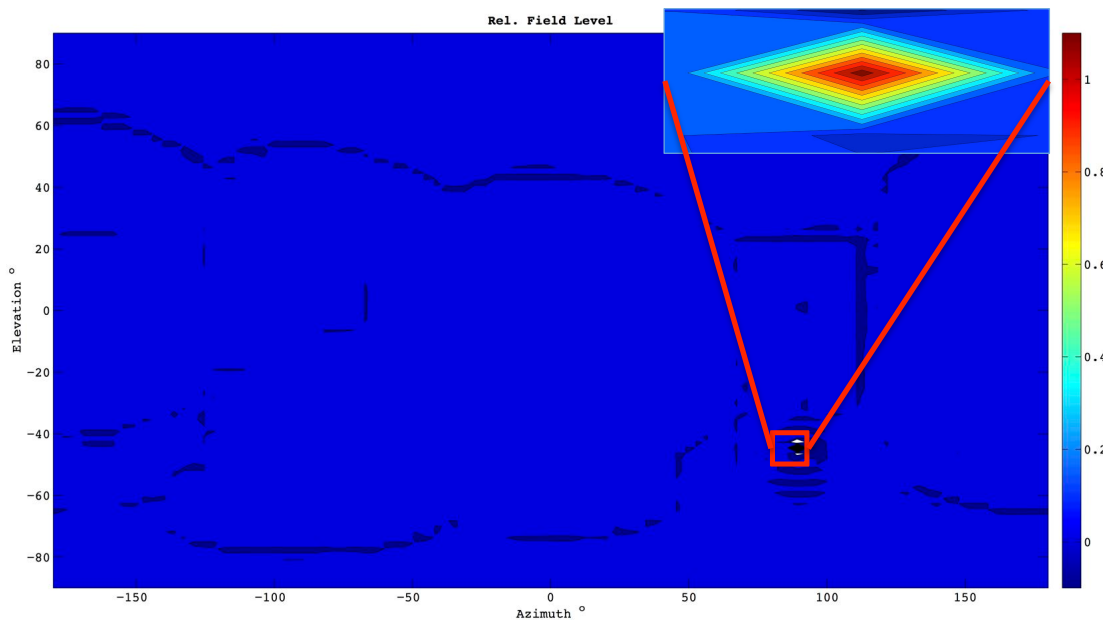


Figure 19 - LOS link for 5.35GHz

From Fig. 18 and 19, it can be seen that the simulator properly finds the LOS link between the two antennas, and a very high peak is observed in both plots, at -45° elevation angle and 90° azimuth angle. The peak's amplitude difference between the signal radiating through the walls or arriving after a number of reflections and the signal that arrives directly from the transmitter is so big that just the LOS link can be seen in the plots.

7.2) Position 1

7.2.1) Measured Results

The measured results for position 1 of the receiver (the position is entitled as "rx" in the measured results provided) can be seen in Fig. 20 and 21. For this position, both FDTD and analytical datasets were tested, in addition with different brick sizes and different cell number.

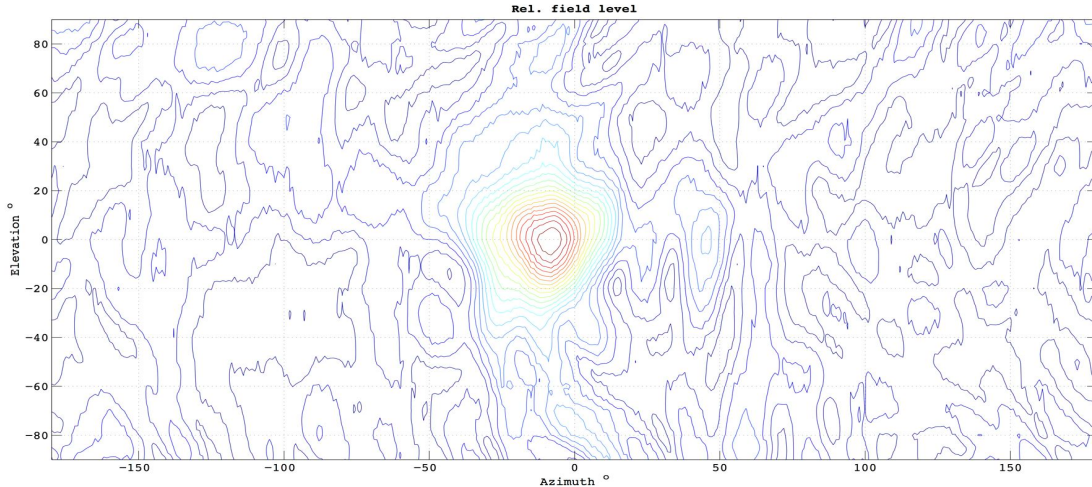


Figure 20 - Measured Result for Position 1 - 5.15GHz

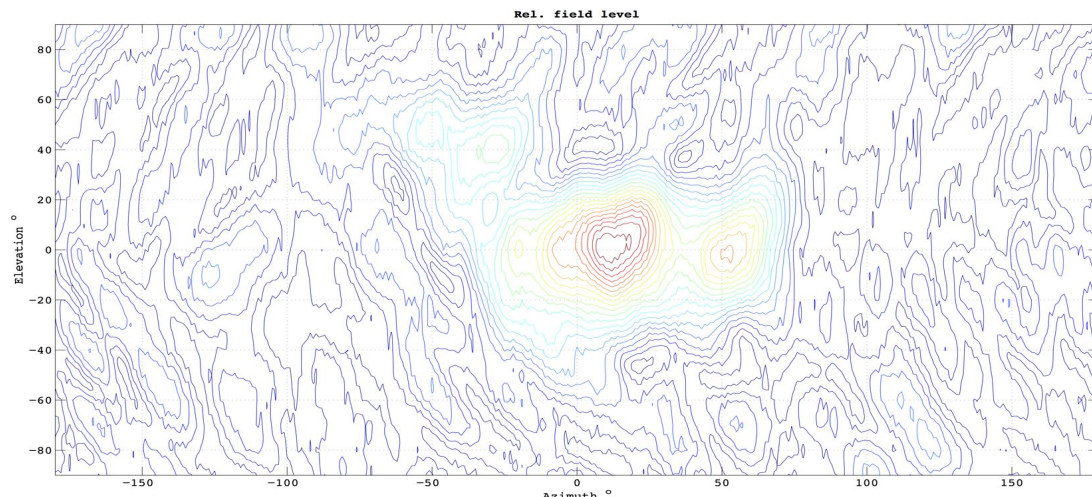


Figure 21 - Measured Result for Position 1 - 5.35GHz

7.2.2) FDTD Method

Firstly, the FDTD – IPO hybrid technique was used for the simulations for both frequencies (Fig. 22 and 23). The number of cells is 100 and the width and height of the brick are 0.2m. As it was previously mentioned, this hybrid method was tested in a previous project of the University of Bristol [9], so the research on that technique will not be extended further using different number of cells and brick sizes. The results of the FDTD simulations are the following:

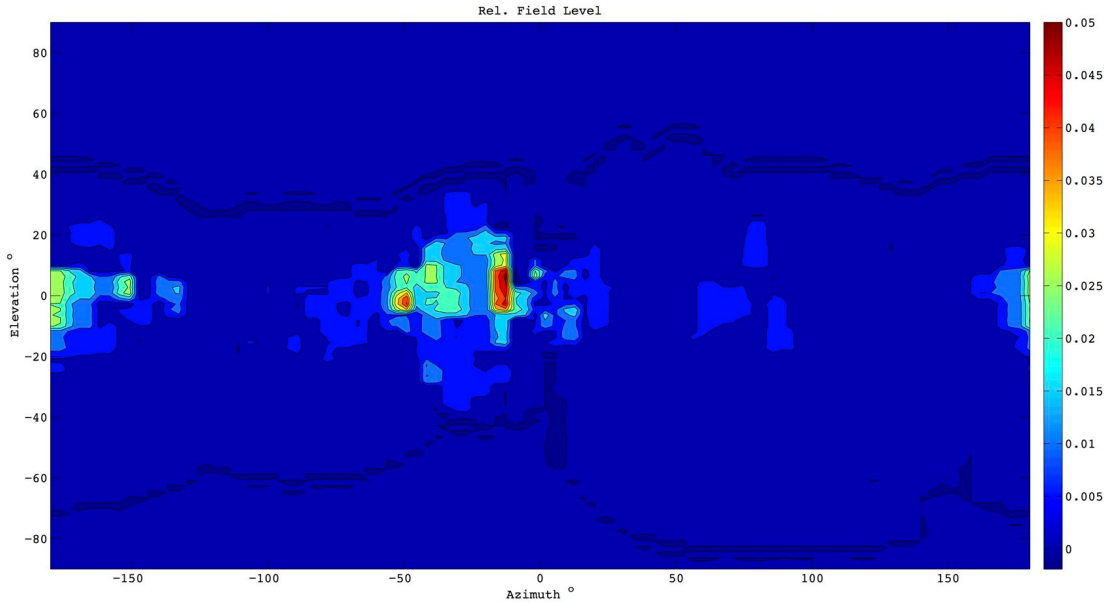


Figure 22 - Position 1 - FDTD Dataset Simulation - 5.15GHz

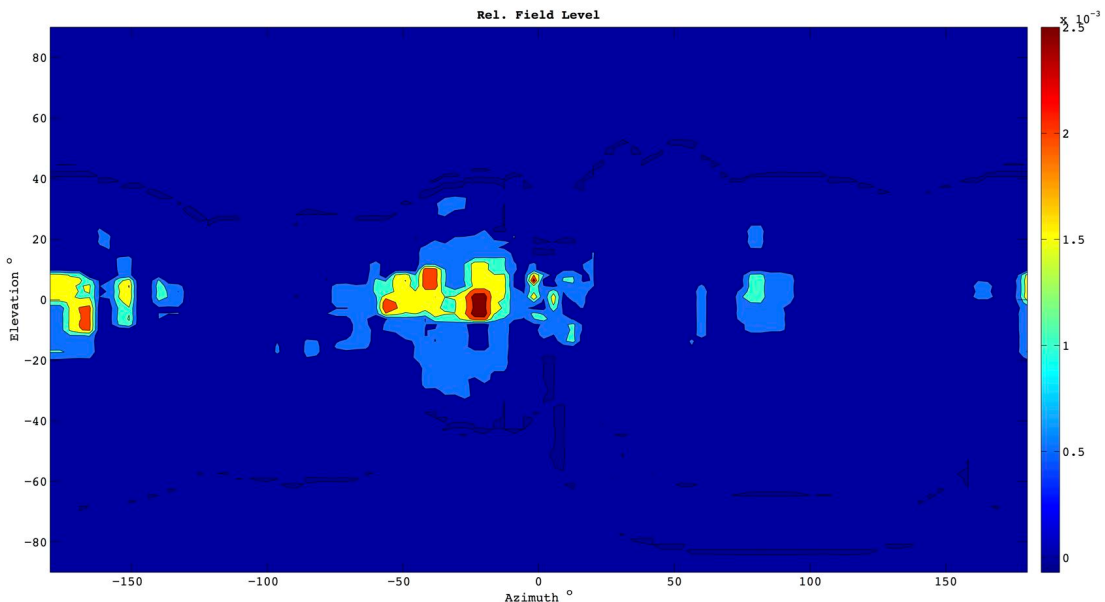


Figure 23 - Position 1 - FDTD Dataset Simulation - 5.35GHz

7.2.3) Analytical Method

7.2.3.1) Analytical Dataset - 5.15 GHz

Using the analytical dataset various simulations took place. Firstly, a brick size of 0.2m in height and width was tested (Fig. 24) with 100 cells. Later, the number of cells was increased to 400 using the same brick size and the simulation was conducted again (Fig. 25). Finally, a smaller brick (Fig. 26) with 100 cells was used (0.1m), to test the effect of the brick size in the simulations.

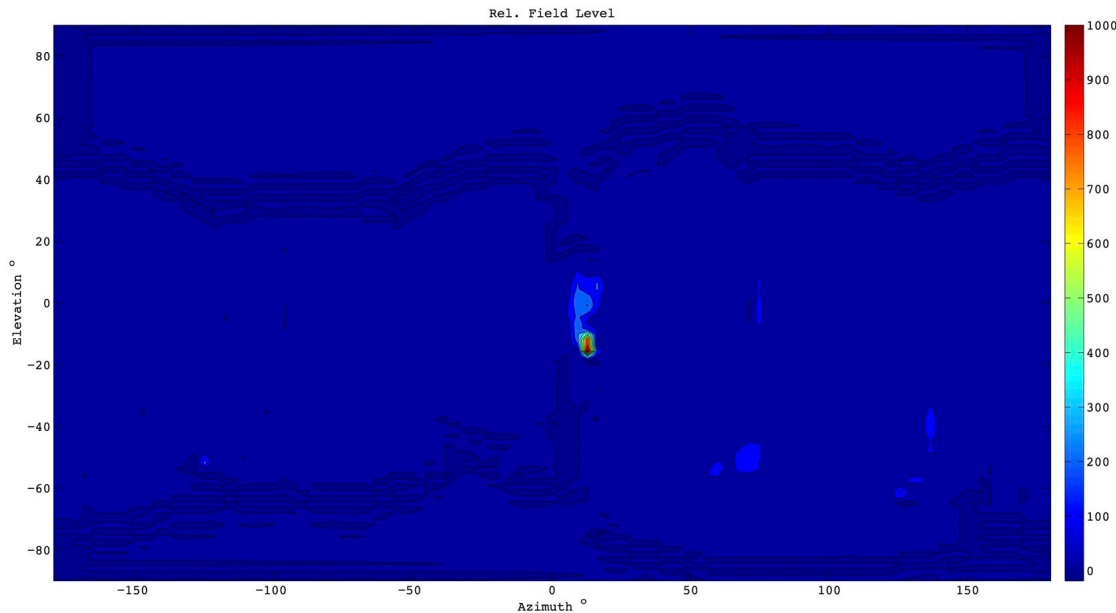


Figure 24 - Position 1 - Larger Brick Simulation - 5.15GHz

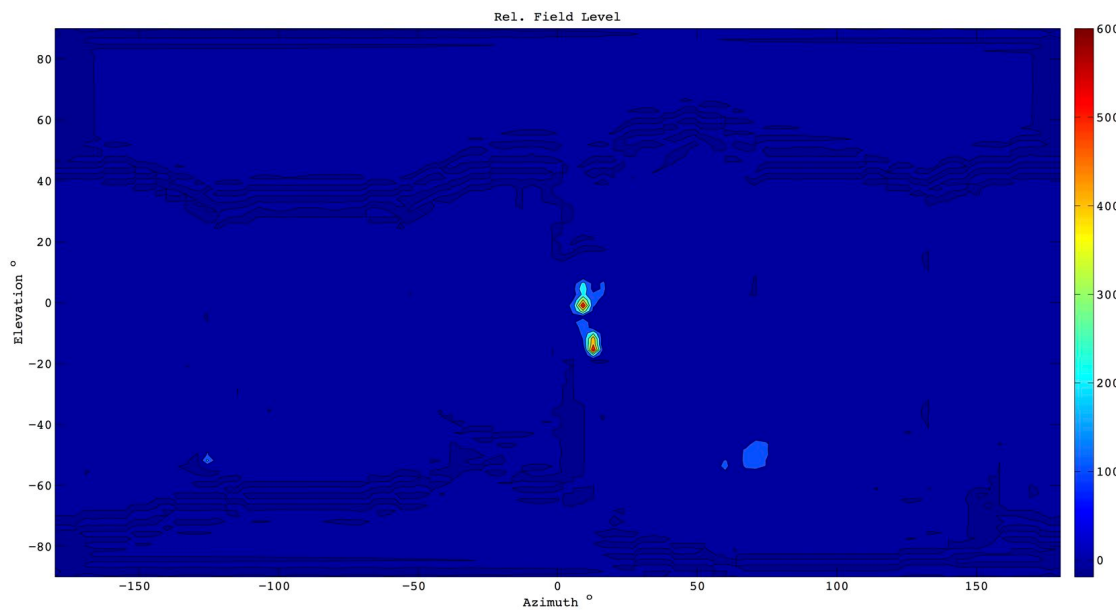


Figure 25 - Position 1 – Larger Number of Cells Simulation - 5.15GHz

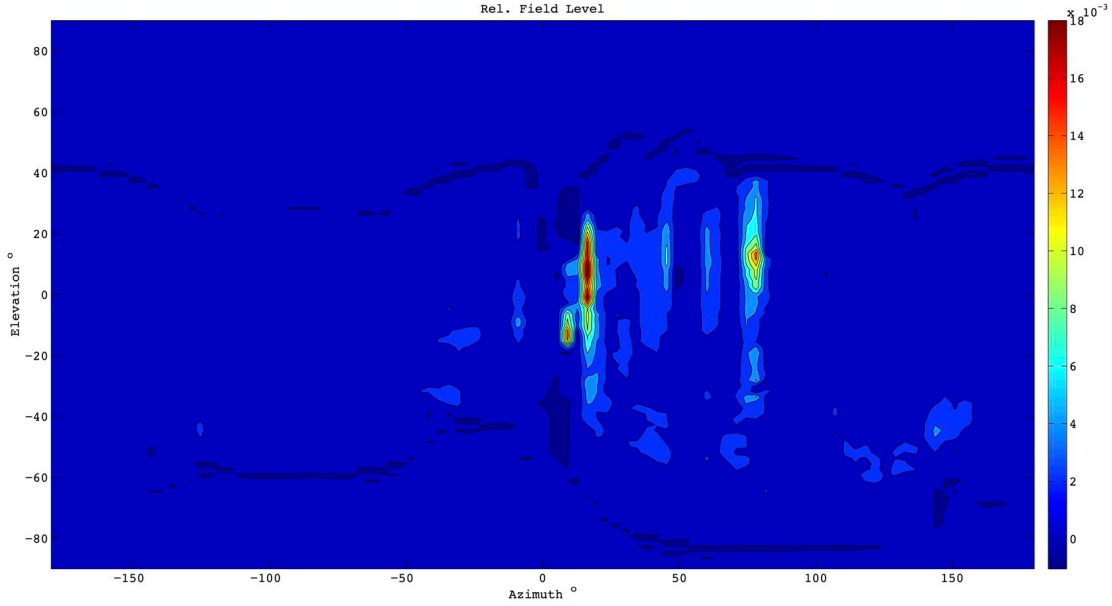


Figure 26 - Position 1 - Smaller brick simulations - 5.15GHz

Comparing the simulated results with the measured ones (Fig. 20) for the simulations conducted at 5.15GHz, it can be seen that both datasets provide accurate results. In the FDTD simulations (Fig. 22), a wrong peak is plotted. On the other hand, in analytical simulations just one peak can be found in almost the same azimuth and elevation angles with the measured results. Slight differences can be seen in the compared results and are a consequence of the approximations made in the program, such as the ideal antenna used for the simulations, the absence of interference from the environment, the lack of knowledge for the specific materials used in the structure and their material properties and finally, the approximations used to reduce the complexity of the simulator.

The simulator faces a drawback when a large brick is used (Fig. 24 and 25). Although, the peak is found in the correct position, the amplitude is very big compared to the one that was expected. As it was aforementioned, the analytical method uses the size of the bricks as an input. The same brick size has to be used for the simulator as well. In the case of a brick size of 0.2x0.2m the gradient calculated from the analytical method is very big. This leads to the software becoming unstable and instead of converging, it scatters, creating this very high peak.

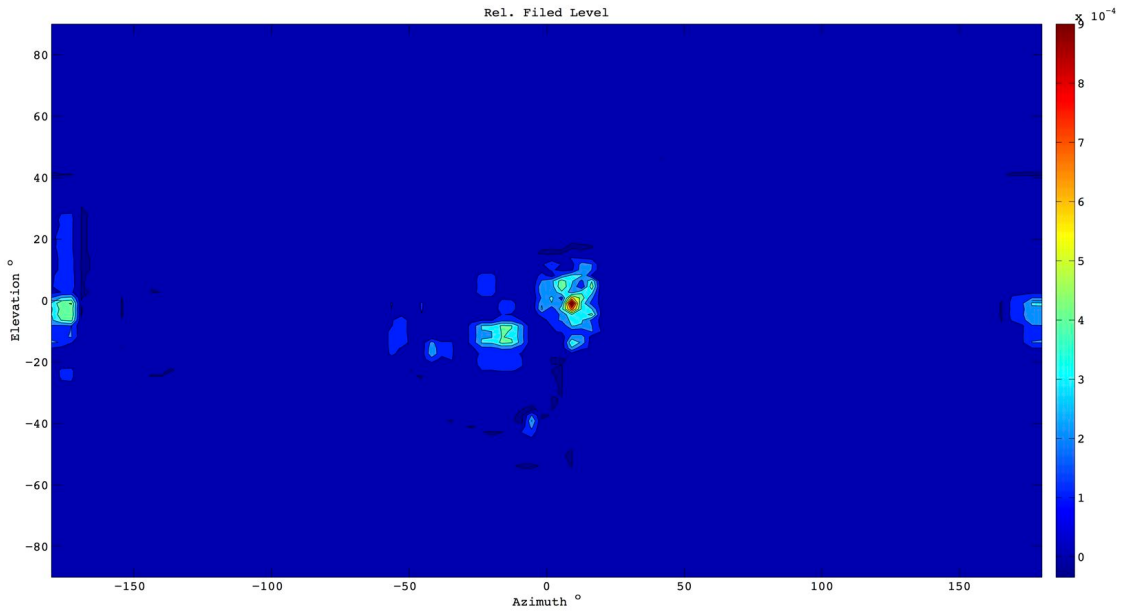


Figure 27 - Position 1 - Non-correlated Brick Size Simulation - 5.15GHz

At that point, experimenting with the values used as an input in the slab3 software, a non-correlated brick size simulation was conducted. The analytical dataset was created using a brick size of 0.1x0.1m and the simulation was conducted using a brick of 0.2x0.2m height and width. The result can be seen in Fig. 27.

Simulations using a non-correlated brick size (Fig. 27) between the two applications give accurate results compared to the measured ones (Fig. 18). So, this might be used as a solution for the previous drawback of the simulator. Nevertheless, despite the results obtained, evidently further investigation is needed on this area.

The different number of cells (Fig. 25) does not change significantly the final result, but it increases quadratically the computational resources and the execution time needed. Consequently, 100 cells are enough for an accurate result. If an extremely accurate result is needed and a way of decreasing the execution time is introduced, then an increased number of cells could be used to improve the accuracy. Finally, the smaller brick size increases the accuracy with expense on the running time.

7.2.3.2) Analytical dataset - 5.35 GHz

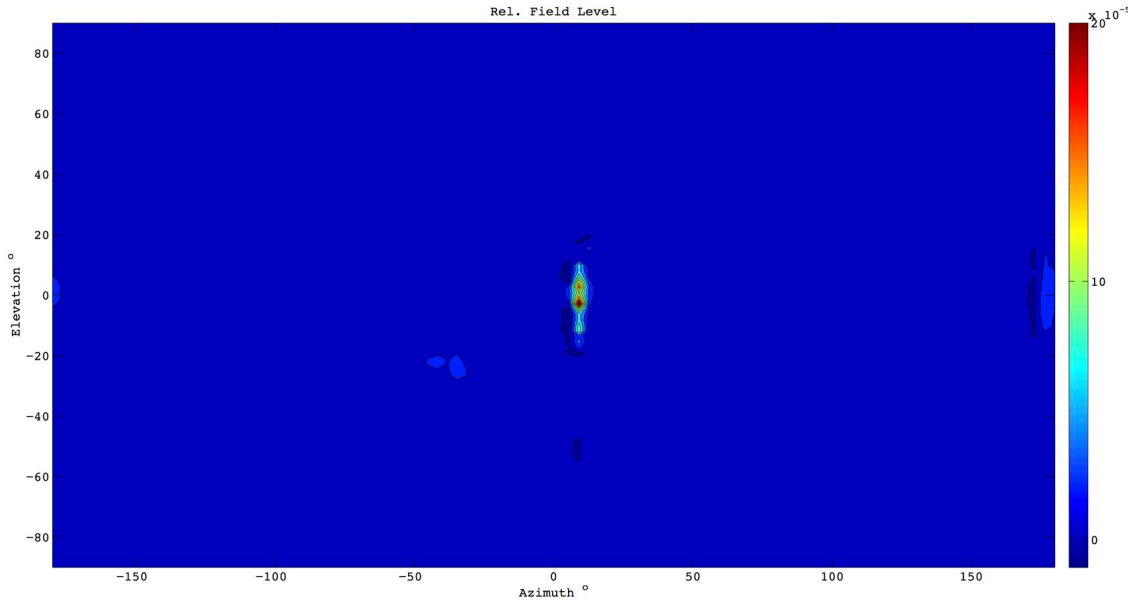


Figure 28 - Position 1 - Smaller Brick Simulation - 5.35GHz

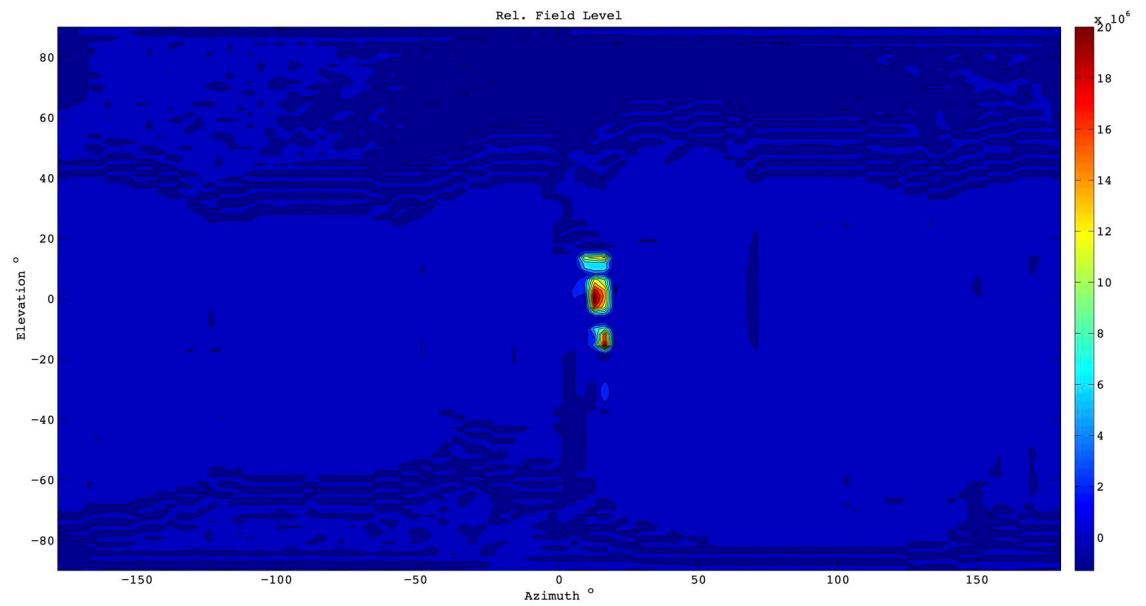


Figure 29 - Position 1 - Larger Brick Scenario - 5.35GHz

For the 5.35GHz scenario, again the simulator predicts accurately the results (Fig. 28 and 29) compared to the measured ones (Fig. 21). When a large brick size is used for the simulation, again the drawback of a very high peak occurs. The smaller brick simulation predicts very accurately the measured results. Finally, using a non-correlated brick size (Fig. 30), returns inaccurate results, thus this approach will be dismissed.

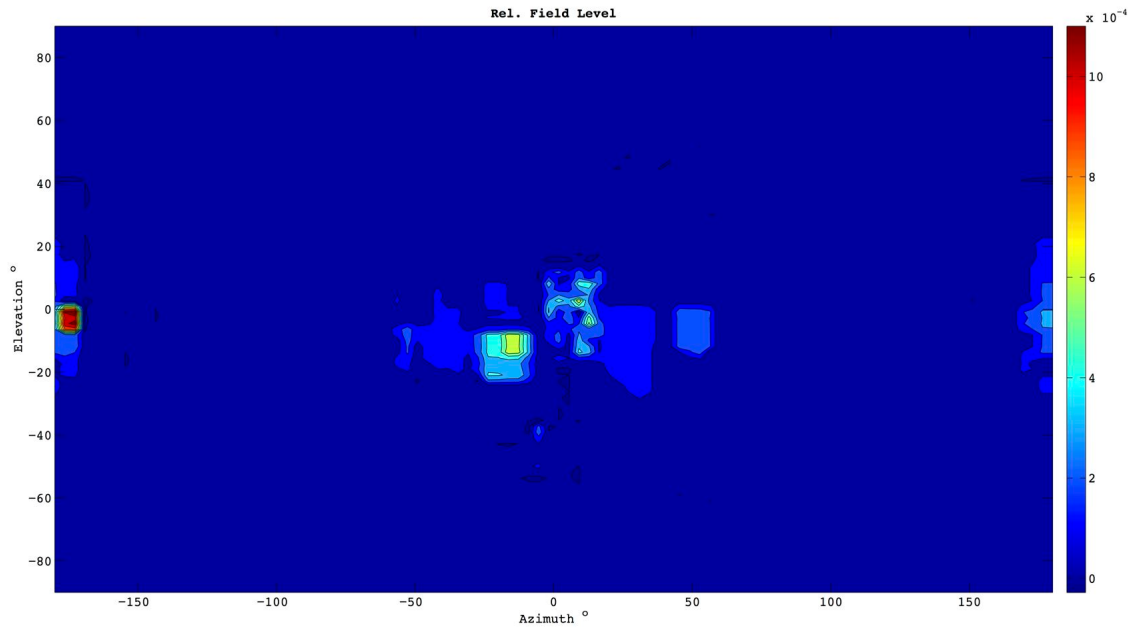


Figure 30 - Position 1 - Non-correlated Brick Size Simulation - 5.35GHz

7.3) Position 2

In order to validate the simulator's accuracy the measured results of two more positions will be compared with the simulated ones. The second position that will be used is named as "rxe" and the measured results provided can be seen in Fig. 31 and 32.

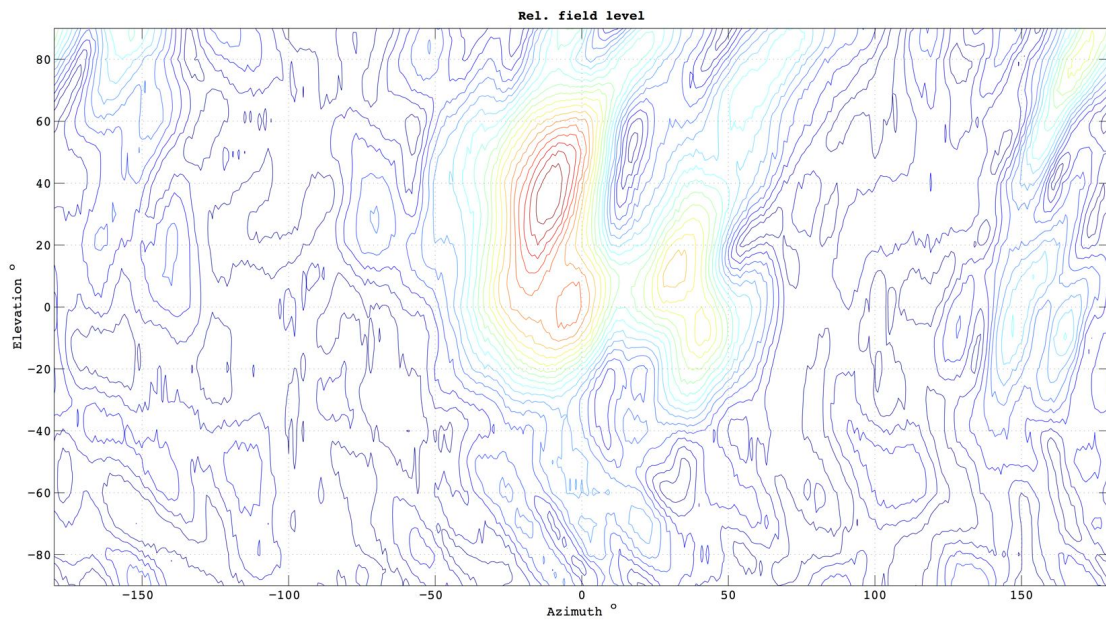


Figure 31 - Measured Results for Position 2 - 5.15GHz

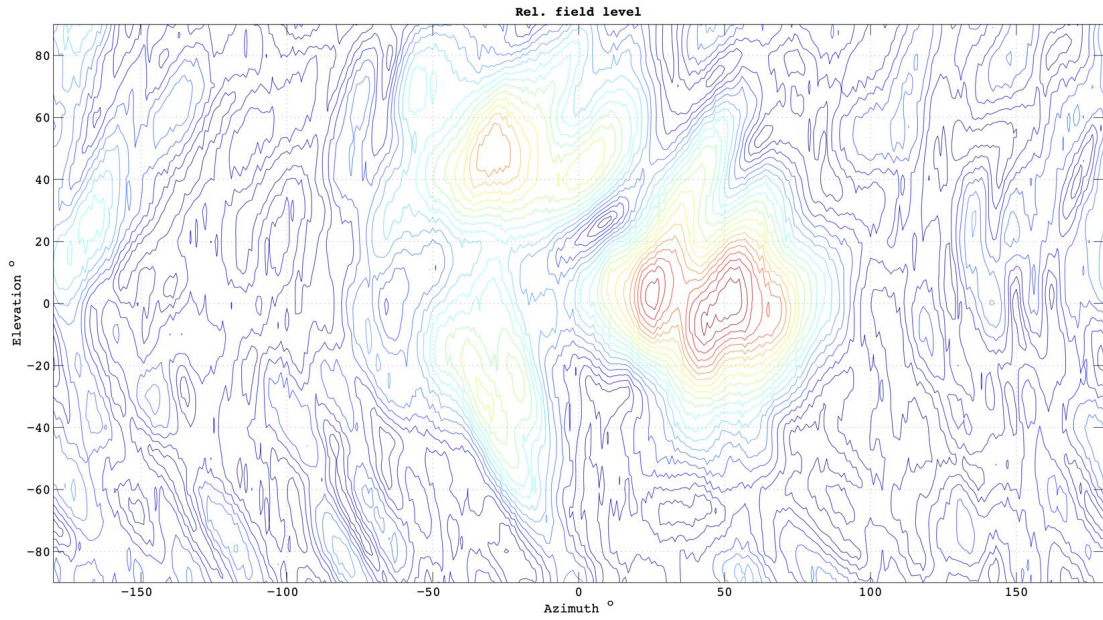


Figure 32 - Measured Result for Position 2 - 5.35GHz

7.3.1) FDTD Method

The hybrid method that combines FDTD and IPO does not predict accurately the results as it can be seen in Fig. 33 and 34 and especially for the 5.35GHz scenario. Again, the same configuration as in Position 1 scenario was used for the simulations.

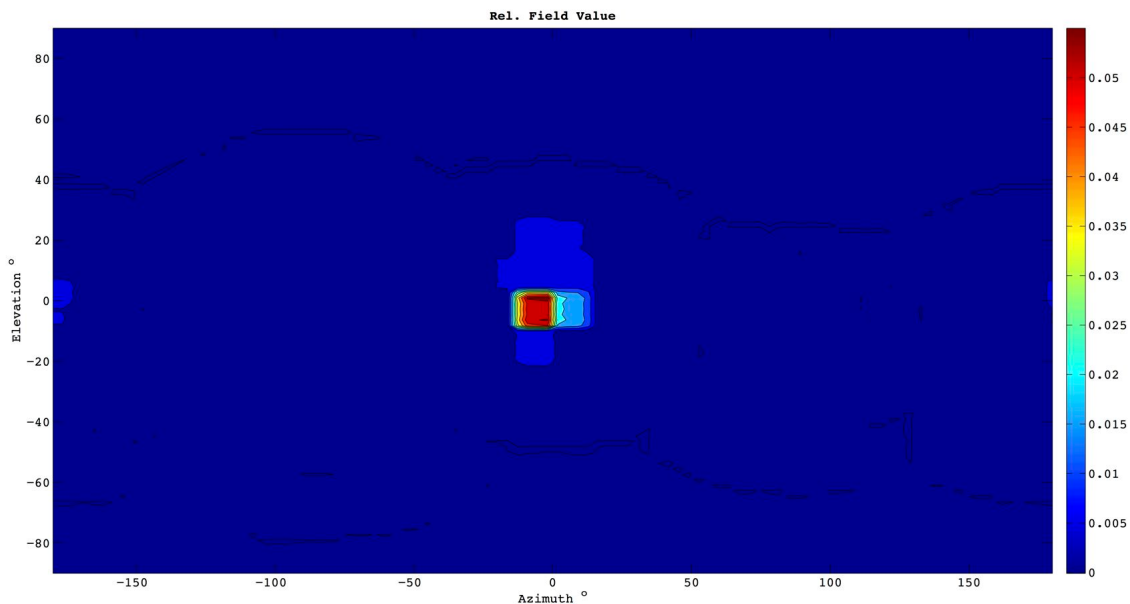


Figure 33 - Position 2 - FDTD Dataset Simulation - 5.15GHz

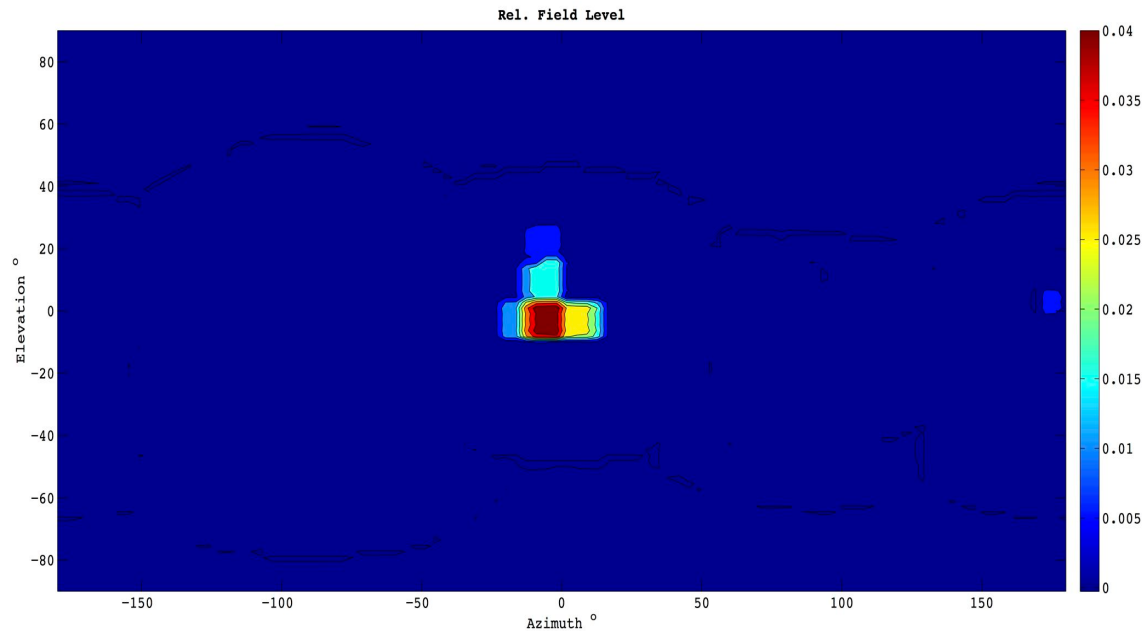


Figure 34 - Position 2 – FDTD Dataset Simulation - 5.35GHz

7.3.2) Analytical Method

7.3.2.1) Analytical Dataset - 5.15GHz

For position 2 and using the Analytical – IPO hybrid method, just the larger and the smaller brick scenarios were simulated. As before, the large brick size is 0.2x0.2m with 100 cells and the small one is 0.1x0.1m with the same number of cells. The results are the following:

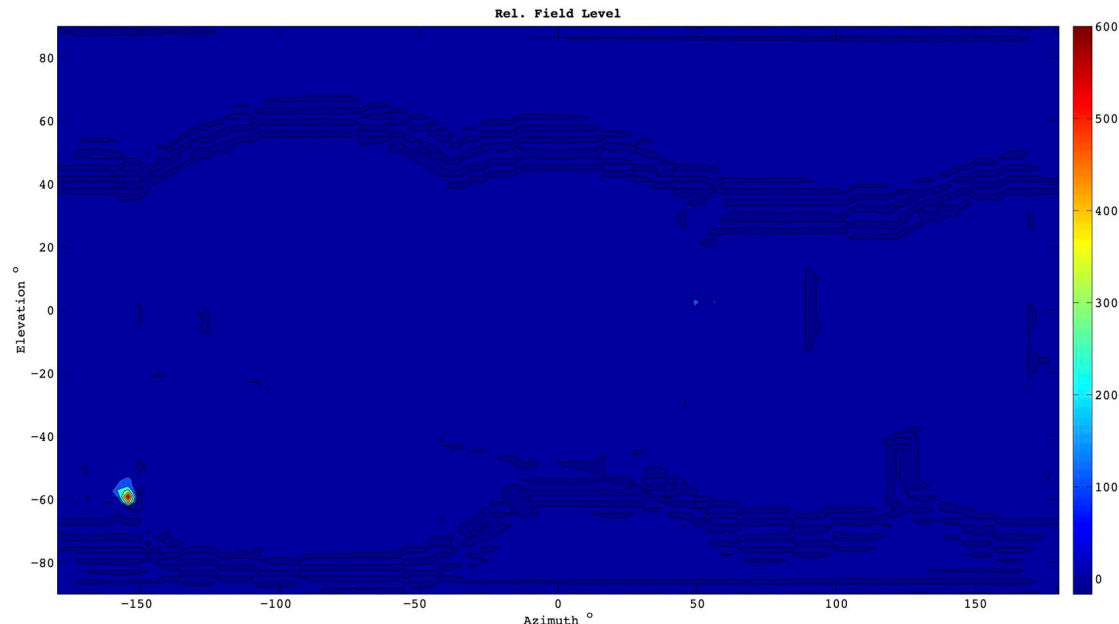


Figure 35 - Position 2 - Larger Brick simulation - 5.15GHz

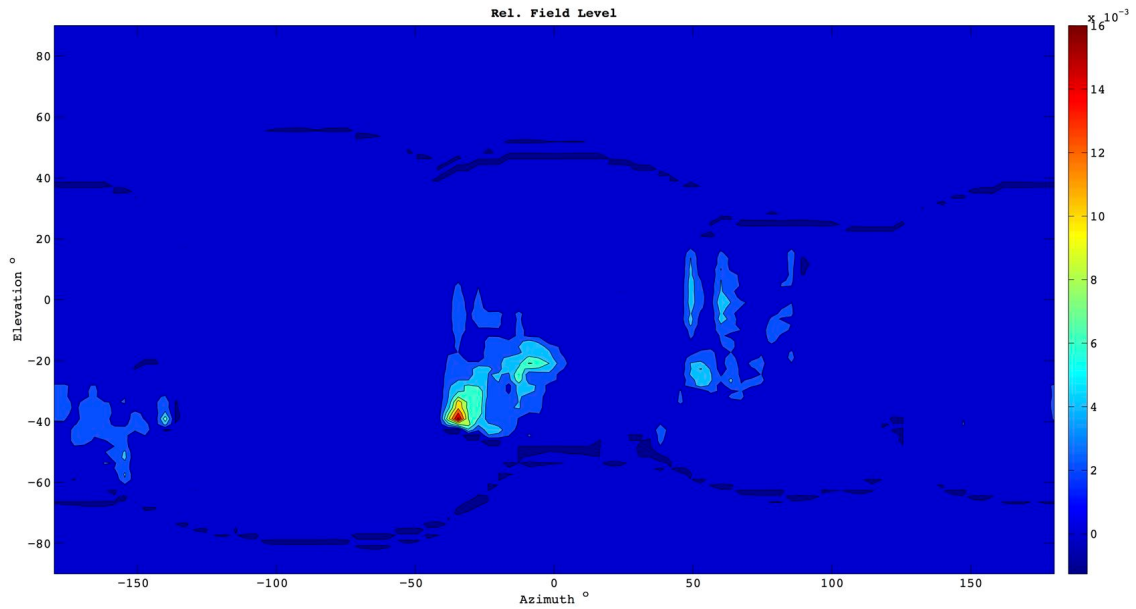


Figure 36 - Position 2 - Smaller Brick Simulation - 5.15GHz

For position 2, the simulated results are not as accurate as the results for position 1. Again, the simulator's drawback is met for a larger brick size (Fig. 35). In addition to that, even the position of the peak is not predicted properly. For the smaller brick scenario (Fig. 34), although the azimuth angle is predicted accurately, the elevation angle shows a discrepancy from the expected result. This is another confirmation that the lack of knowledge for the materials used and their properties leads to inaccuracy in the simulations.

7.3.2.2) Analytical Dataset – 5.35GHz

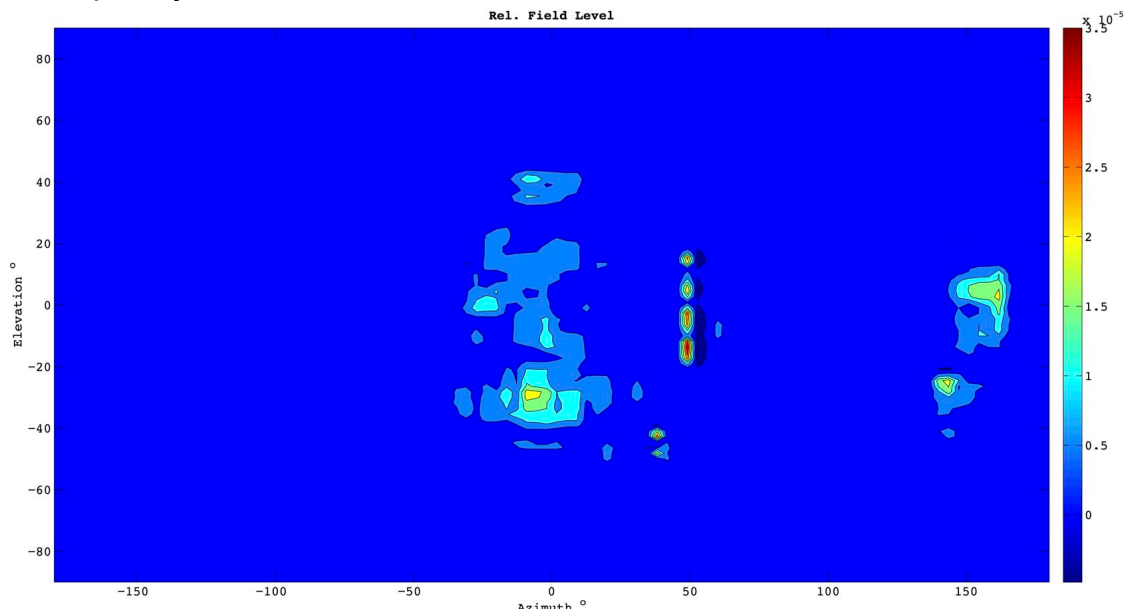


Figure 37 - Position 2 - Smaller Brick Simulation - 5.35GHz

Conducting a simulation with a smaller brick at 5.35GHz (Fig. 37), it is shown that again the simulator predicts accurately the direction of the strongest signal.

7.4) Position 3

The final position used is the one entitled as “rxf” and the measured results can be seen in the relevant figure (Fig. 38). As it was observed from the previous simulations, the most accurate results are shown when a smaller brick size is used with the analytical method. Thus, for this position, just this scenario will be tested in order to validate the simulator’s accuracy.

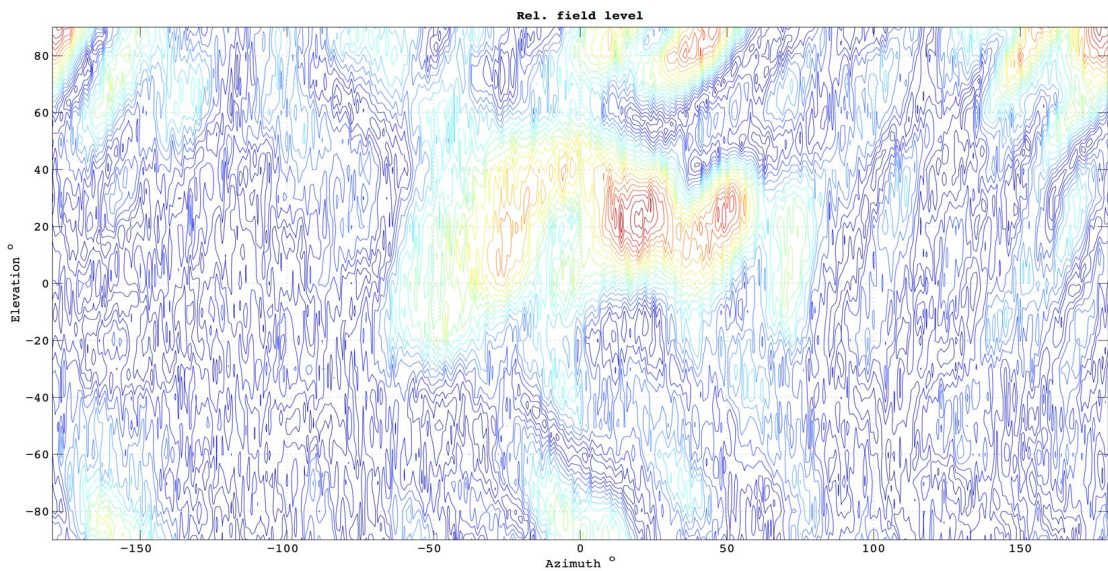


Figure 38 - Measured Result for Position 3 - 5.15GHz

7.4.1) Analytical Method

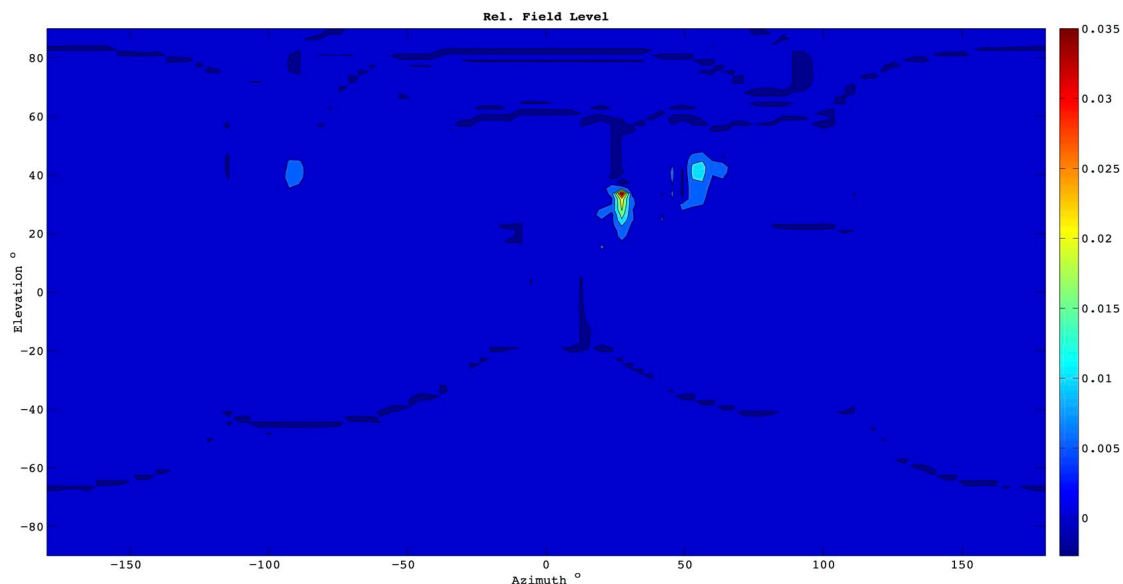


Figure 39 - Position 3 - Small Brick Simulation - 5.15GHz

The simulator accurately predicted the peak for position 3. From Fig. 38, it can be seen that the strongest signal comes from about 20° of Azimuth angle and about 30° of elevation angle, something that matches with the measured results (Fig. 38).

7.5) Improved Performance

The optimised code decreases the execution time of the IPO3 software. The previous version of the software needed more than 10 hours for a simple simulation on a computer with a CPU Intel Core i7 2GHz, 4 GB of RAM memory and OS X 10.9.4 operating system. After the optimisation, about 6-7 hours are needed for the same simulation. The simulation used for this experiment used the FDTD method, because the algorithm is almost identical with the one used in the previous version of the software. Therefore, the complexity of the software was not increased and thus any change in the execution time is a result of only the optimisation. IPO_AoA executes in about 40-60s depending on the size of the “.prn” files and using the same optimisation techniques for that application as before, the execution time was improved about 40% as well.

Introducing the convergence threshold in the simulations, the execution time is decreased even more and about 4 hours are needed for a complete simulation. Taking into account the drawback of the simulation that was mentioned before, and the instability that is caused because of this drawback, it was considered better to restrict this convergence rule just for the FDTD method.

7.6) Reflection coefficients and Frequency

Additionally to the previous simulations, it was observed that a ray's reflection from a wall varies rapidly with the frequency. A typical reflection coefficient plot in dependence with the frequency can be seen in Fig. 40.

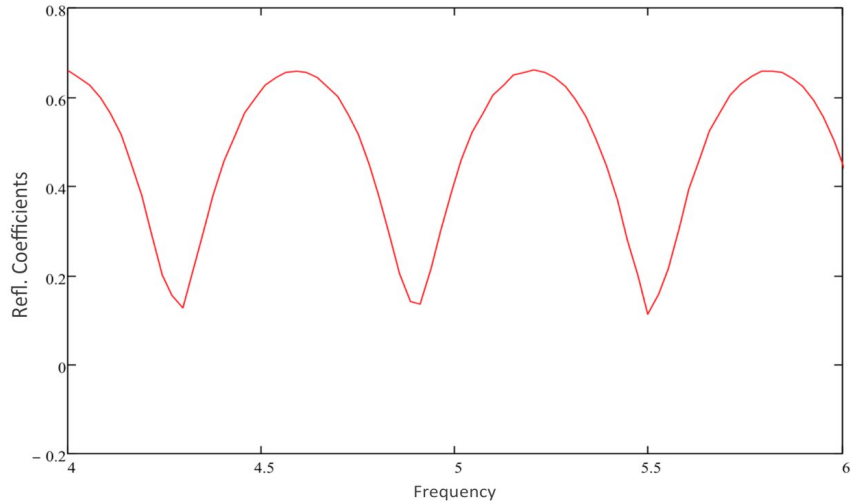


Figure 40 - Typical Reflection Coefficient Plot

In order to check if slightly different frequencies change significantly the simulated result two more simulations were conducted at 5GHz and 5.5GHz for position 1. A smaller brick size was used for the simulations and 100 cells. As it can be seen from Fig. 40, the variation in the reflection coefficients between these two frequencies can cover all the changes from the lowest to the highest values of the reflection coefficient. The results for these two simulations can be seen in Fig. 41 and 42. Comparing these results with the ones found at 5.15GHz and 5.35GHz (Fig. 26 and 28), it can be seen that even though the reflection coefficients change significantly regarding frequency the results are similar for all the frequencies. This is because multiple rays transmitted and reflected are considered in order to calculate the final result, therefore this variation negligibly affects the results.

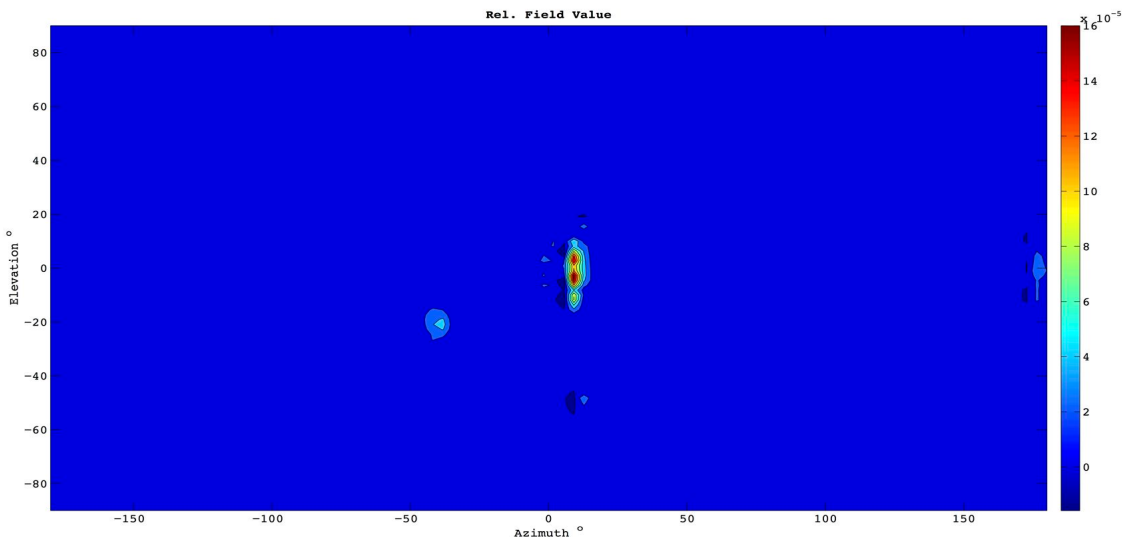


Figure 41 - Reflection Coefficients and Frequency Dependence - 5GHz

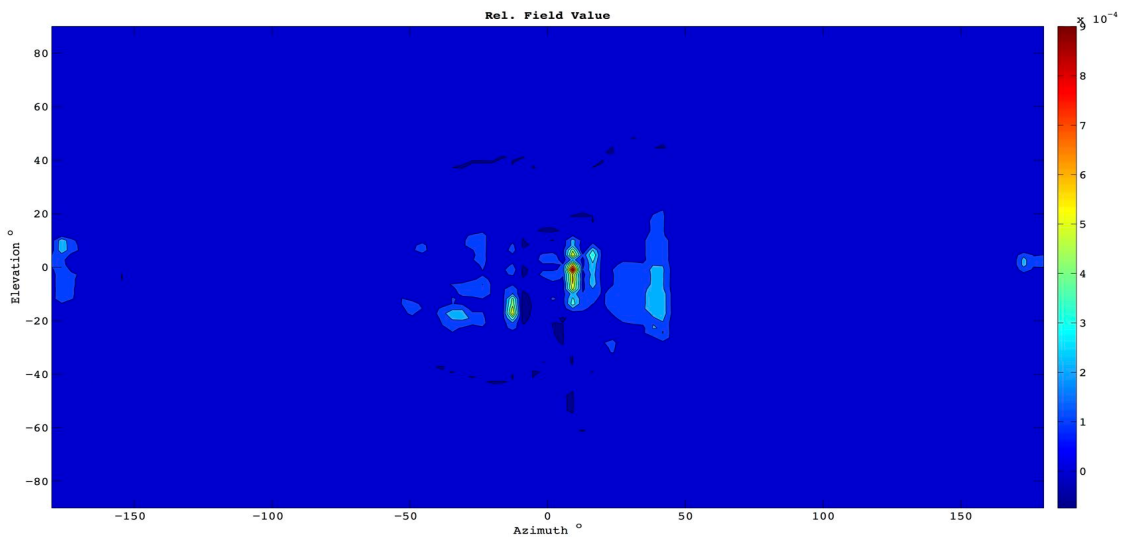
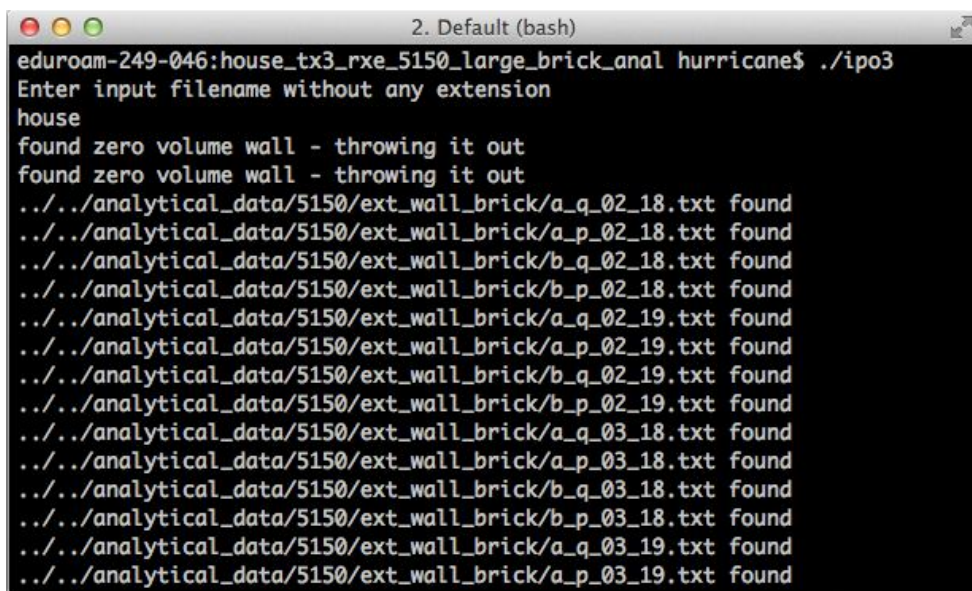


Figure 42 - Reflection Coefficients and Frequency Dependence – 5.5GHz

8) How to use the software

All the input files described before, must be in the same folder. For this project, the input filename used was “*house*”, as is the name of the file containing the wall coordinates and objects.

IPO3 is the first software that needs to be executed. There are two different ways of running the software. The first one is using the integrated function of Lazarus IDE and run the “ipo3.lpr”. When a terminal window pops up, the string “*house*” is given as an input following the software steps and the simulation starts. If Lazarus IDE is not installed, the executable files generated can be used. The files generated, can be used with all the Unix-based computers (Fig. 43). Some examples of the time needed to conduct the simulations were presented earlier in this report.

A screenshot of a terminal window titled "2. Default (bash)". The window shows the command "eduroam-249-046:house_tx3_rxe_5150_large_brick_anal hurricane\$./ipo3" followed by the string "house". The output of the program is displayed below, showing the search path for zero-volume walls and found files in the "analytical_data/5150/ext_wall_brick/" directory.

```
2. Default (bash)
eduroam-249-046:house_tx3_rxe_5150_large_brick_anal hurricane$ ./ipo3
Enter input filename without any extension
house
found zero volume wall - throwing it out
found zero volume wall - throwing it out
....../analytical_data/5150/ext_wall_brick/a_q_02_18.txt found
....../analytical_data/5150/ext_wall_brick/a_p_02_18.txt found
....../analytical_data/5150/ext_wall_brick/b_q_02_18.txt found
....../analytical_data/5150/ext_wall_brick/b_p_02_18.txt found
....../analytical_data/5150/ext_wall_brick/a_q_02_19.txt found
....../analytical_data/5150/ext_wall_brick/a_p_02_19.txt found
....../analytical_data/5150/ext_wall_brick/b_q_02_19.txt found
....../analytical_data/5150/ext_wall_brick/b_p_02_19.txt found
....../analytical_data/5150/ext_wall_brick/a_q_03_18.txt found
....../analytical_data/5150/ext_wall_brick/a_p_03_18.txt found
....../analytical_data/5150/ext_wall_brick/b_q_03_18.txt found
....../analytical_data/5150/ext_wall_brick/b_p_03_18.txt found
....../analytical_data/5150/ext_wall_brick/a_q_03_19.txt found
....../analytical_data/5150/ext_wall_brick/a_p_03_19.txt found
```

Figure 43 - IPO3 execution and string input

When IPO3 algorithm is finished, IPO_AoA (Fig. 44) software is used to find the energy arriving at the receiver. This program, is a lot faster compared to the previous one, and needs between a few seconds and 1 minute to end. The final text file that is created (Fig. 45) is plotting in Matlab using “plotting.m” program.

```
2. Default (bash)
eduroam-249-046:house_tx3_rxf_5150_small_brick_hurricane$ ./ipo_AoA
Enter input filename without any extension
house
found zero volume wall - throwing it out
found zero volume wall - throwing it out
_3.prn
reading file house_wall01_3.prn
reading file house_wall02_3.prn
reading file house_wall03_3.prn
reading file house_wall04_3.prn
reading file house_wall05_3.prn
reading file house_wall06_3.prn
reading file house_wall07_3.prn
reading file house_wall08_3.prn
reading file house_wall09_3.prn
reading file house_wall10_3.prn
reading file house_wall11_3.prn
reading file house_wall12_3.prn
reading file house_wall13_3.prn
```

Figure 44 - IPO_AoA execution and string input

```
2. Default (ipo_AoA)
elevation -7.000000E+0001
elevation -7.200000E+0001
elevation -7.400000E+0001
elevation -7.600000E+0001
elevation -7.800000E+0001
elevation -8.000000E+0001
elevation -8.200000E+0001
elevation -8.400000E+0001
elevation -8.600000E+0001
elevation -8.800000E+0001
elevation -9.000000E+0001
distance: 5.42000000000000E+000 -6.00000000000000E-001 2.55000000000000E+
000
rhat: 9.00350858989739E-001 -9.96698367885320E-002 4.23596806351261E-001
theta: 1.1333840371315148E+0000 theta degree: 6.4938121895134376E+0001
phi: 6.1729331082597690E+0000 phi degree: -6.3169856801423551E+0000
emag_h: 0.00000000000000E+0000
The program has finished
```

Figure 45 - IPO_AoA execution end and final text file created

9) Conclusions

For the purposes of this project, a software application that predicts the propagation characteristics for an indoor scenario consisted of a complex layout and lossy materials was implemented. The arriving energy was modelled using two hybrid techniques that combine IPO with FDTD and an analytical method. IPO is beneficial compared to other techniques, due to the increased accuracy and the average computational resource needs

The simulator was able to predict accurately the wave propagation for various antennas' positions, including the scenario that the two antennas have LOS between them. Using the hybrid method that combines IPO with FDTD, only one type of material was taken into account. Consequently, even though the results are promising, they are less accurate compared to the second hybrid technique.

Using the analytical method, various simulations with different brick sizes and different number of cells were conducted. From the results, it was concluded that a smaller brick size enhances the accuracy of the simulator. On the other hand, an increased number of cells mostly increase the computational resources and the execution time needed. One drawback appeared during the simulations and it has to do with the correlation of the brick size used in the simulator and the analytical method.

Regarding the optimisation of the code, the execution time is decreased about 30-40% using the analytical hybrid method and almost 60% using FDTD method due to the convergence rule taken into account.

In conclusion, this simulator is working accurately. This project provides a tool for studying the effect of a complex lossy structure in an indoor propagation scenario. Different factors that affect the radiation of a ray are take into account, such as the position of the antennas, the materials used for the building, the number of objects, and the frequency, without the need of experimentation using physical, pricey equipment.

10) Future Work

The degree of accuracy can be increased with research on the building materials and their properties. At first, a research like this should provide better understanding of the objects and the materials used inside a building and ensuing material properties should be investigated for the various frequencies that an antenna works during an indoor scenario.

In addition to that, a series of simulations similar to the ones conducted using the analytical method, but instead using the FDTD method, to calculate the radiation inside the various objects and materials, could be a possible path for future research. This will probably increase the accuracy of the simulator, in the expense of the very long time, needed at first to simulate the FDTD results.

Another step is trying to improve the drawback that was discovered while using the analytical method and large bricks. Slab3 software needs to be improved in order to avoid leading to this instability during the simulations and the very high peaks that were seen in the results.

Finally, IPO algorithm is parallelizable. Using multithreading programming and making the software feasible to run on parallel processors, will imply to additional computational advantages and give the chance of even more complex structures to be used in the future.

References

- [1] C. Balanis, *Advanced Engineering Electromagnetics*, 2nd ed. Wiley & Sons, 2012.
- [2] P. Y. Ufimtsev, *Fundamentals of the physical theory of diffraction*. John Wiley & Sons, Inc., 2006.
- [3] F. Obelleiro-Basteiro, J. L. Rodriguez, and R. J. Burkholder, "An Iterative Physical Optics Approach for Analyzing the Electromagnetic Scattering by Large Open-Ended Cavities," *Antennas Propag. IEEE Trans. On*, vol. 43, no. 4, pp. 356 – 361, Apr. 1995.
- [4] R. J. Burkholder, C. Tokgoz, C. J. Reddy, and P. H. Pathak, "Iterative physical optics: its not just for cavities anymore," in *Antennas and Propagation Society International Symposium, 2005 IEEE*, 2005, vol. 1A, pp. 18–21 Vol. 1A.
- [5] F. Obelleiro, J. Campos-Ninō, J. L. Rodriguez, and A. G. Pino, "A Segmented Approach for Computing the Electromagnetic Scattering of Large and Deep Cavities," *J. Electromagn. Waves Appl.*, vol. 12, no. 9, pp. 129–145, Jan. 1998.
- [6] F. Obelleiro, M. G. Araújo, and J. L. Rodriguez, "Iterative physical-optics formulation for analyzing large waveguides with lossy walls," *Microw. Opt. Technol. Lett.*, vol. 28, no. 1, pp. 21–26, Jan. 2001.
- [7] M. G. Araújo, F. Obelleiro, and J. L. Rodriguez, "Modeling High Frequency Propagation in Tunnel Environments by Iterative Physical Optics Method," *Wirel. Pers. Commun.*, vol. 20, no. 3, pp. 237–250, Mar. 2002.
- [8] "IPO propagation Programs Handbook (IPO3, IPO_AoA, IPO_verify, write_svg)." University of Bristol, 2013.
- [9] G. Hou, "Propagation Modeling by using Iterative Physical Optics," University of Bristol, Department of Electrical & Electronic Engineering, 2013.
- [10] Y. Wang, S. Safavi-Naeini, and S. K. Chaudhuri, "A Hybrid Technique Based on Combining Ray Tracing and FDTD Methods for Site-Specific Modeling of Indoor Radio Wave Propagation," *Antennas Propag. IEEE Trans. On*, vol. 48, no. 5, pp. 743–754, May 2000.
- [11] M. Thiel and K. Sarabandi, "A Hybrid Method for Indoor Wave Propagation Modeling," *Antennas Propag. IEEE Trans. On*, vol. 56, no. 8, pp. 2703–2709, Aug. 2008.

- [12] S. Reynaud, Y. Cocheril, R. Vauzelle, A. Reineix, L. Aveneau, and C. Guiffaut, "Influence of an accurate environment description for the indoor propagation channel modelling," in *Wireless Technology, 2005. The European Conference on*, 2005, pp. 51–54.
- [13] A. Taflove and S. C. Hagness, *Computational Electrodynamics: The Finite-Difference Time-Domain Method*, 3rd ed. Artech House, Inc., 2005.
- [14] H. Ling, R. Choo, and S.-W. Lee, "Shooting and Bouncing Ray: Calculating the RCS of an Arbitrarily Shaped Cavity," *Antennas Propag. IEEE Trans. On*, vol. 37, no. 2, pp. 194–205, Feb. 1989.
- [15] R. J. Burkholder, R.-C. Chou, and P. H. Pathak, "Two ray shooting methods for computing the EM scattering by large open-ended cavities," *Comput. Phys. Commun.*, vol. 68, no. 1, pp. 353–365, May 1991.
- [16] J. L. Rodriguez, F. Obelleiro, and A. G. Pino, "Iterative solutions of MFIE for computing electromagnetic scattering of large open-ended cavities," *Microw. Antennas Propag. IEE Proc.*, vol. 144, no. 2, pp. 141–144, Apr. 1997.
- [17] Y. Oh, "An Exact Evaluation of Kirchhoff Approximation for Backscattering from a One-Dimensional Rough Surface," in *Antennas and Propagation Society International Symposium, 1996. AP-S. Digest*, 1996, vol. 2, pp. 1522–1525.
- [18] "Free Pascal - Advanced open source Pascal compiler for Pascal and Object Pascal." [Online]. Available: <http://www.freepascal.org/>. [Accessed: 11-Apr-2014].
- [19] "Programming languages performance ranking - Dr. Joey Paquet Web Site." [Online]. Available: http://users.encs.concordia.ca/~paquet/wiki/index.php?title=Programming_languages_performance_ranking. [Accessed: 11-Apr-2014].
- [20] "Free Pascal Lazarus IDE." [Online]. Available: <http://www.lazarus.freepascal.org/>. [Accessed: 11-Mar-2014].
- [21] P. Zhang, "Propagation Modeling using Iterative Physical Optics," University of Bristol, Department of Electrical & Electronic Engineering, 2011.
- [22] "External Wall Building Regulations," *Planning Portal - The UK Government's online planning and building regulations resource*. [Online]. Available:

<http://www.planningportal.gov.uk/permission/commonprojects/externalwalls>. [Accessed: 13-Aug-2014].

- [23] "Cavity Walls," *Sustainable Building Solutions*, 2011. [Online]. Available: <http://www.sustainablebuildingsolutions.co.uk/solution-data-sheets/cavity-walls-fully-filled>. [Accessed: 13-Aug-2014].
- [24] "Optim-R External Wall System - Next Generation Insulation for Masonry Walls." Kingspan, Jul-2013.
- [25] I. Cuiñas and M. G. Sánchez, "Permittivity and Conductivity Measurements of Building Materials at 5.8 GHz and 41.5 GHz," *Wirel. Pers. Commun.* 20, pp. 93–100, 2002.
- [26] A. Muqaibel, A. Safaai-Jazi, A. Bayram, A. M. Attiya, and S. M. Riad, "Ultrawide-band through the wall propagation," *Microw. Antennas Propag. IEEE Proc.*, pp. 581–588, Dec. 2005.
- [27] I. Cuiñas, J.-P. Pugliese, A. Hammoudeh, and M. G. Sanchez, "Frequency Dependence of Dielectric Constant of Construction Materials in Microwave and Millimeter-Wave Band," *Inc Microw. Opt Technollett 30 John Wiley Sons*, pp. 123–124, 2001.
- [28] Y. Pinhasi, A. Yahalom, and S. Petnev, "Propagation of Ultra Wide-Band Signals in Lossy Dispersive Media," *Microw. Commun. Antennas Electron. Syst. 2008 COMCAS 2008 IEEE Int. Conf.*, pp. 1–10, May 2008.
- [29] C. Balanis, *Antenna Theory: Analysis and Design*, Third. USA: Wiley - Interscience, 2005.
- [30] "Half-Wavelength Dipole Antenna," *The Antenna Theory Website*. [Online]. Available: <http://www.antenna-theory.com/antennas/halfwave.php>. [Accessed: 12-Aug-2014].